Groundwater use for agricultural production - current water budget and expected trends under climate change

FINAL REPORT

Marie Larocque
Jana Levison
Sylvain Gagné
Shoaib Saleem

UNIVERSITÉ DU QUÉBEC À MONTRÉAL and UNIVERSITY OF GUELPH

August 30, 2019

Reference to be cited

Larocque, M., J. Levison, S. Gagné, S. Saleem. 2019. Groundwater use for agricultural production – current water budget and expected trends under climate change. Final report submitted to MAPAQ and OMAFRA. Université du Québec à Montréal and University of Guelph. Montréal (Québec) and Guelph (Ontario). 67 p.

SUMMARY

Global changes from natural and anthropogenic sources (e.g. climate change, population growth, agricultural intensification) place great stress on water resources. Groundwater resources are of great importance for rural communities and for agricultural production in southern Ontario, Canada. The goal of this research was to improve the understanding of potential opportunities and challenges for the agricultural industry relying on groundwater resources in a changing climate. This was accomplished through quantifying the water budget in a water-stressed agriculturally-dominated area and examining the long-term sustainability of groundwater source availability for agriculture, considering future climate stresses and potential land use changes. In the lower portion of the Whitemans Creek subwatershed, part of the Grand River watershed, Ontario, a detailed analysis of the water budget, including collection of field data and numerical simulations using the coupled SWAT-MODFLOW model, was conducted. The water budget analysis indicates that recharge is the main component of the water cycle followed by evapotranspiration. Groundwater discharge to the stream calculated using a digital filter is between 0.34 and 1.25 m^3/s with a median of 0.73 m^3/s (159 and 585 mm/yr; median of 344 mm/yr). Reported groundwater use is low in the subwatershed, but allowed (permitted) amounts are close to mean annual recharge. In 2016, for example, the LWC had 47 active PTTW, pumping the aquifer (12 permits), ponds (32 permits) and surface water (3 permits) for the equivalent of 182 mm/yr. Agricultural use accounts for >95% of the permitted pumping. However, the maximum declared water use was 18 mm/yr in 2012. Modeling results from SWAT (surface model only), for the past conditions, gives a mean annual recharge of 424 mm. Simulated baseflow from SWAT for the past condition is 390 mm (0.79 m^3/s) while the baseflow simulated by the SWAT-MODFLOW model is 236 mm (0.49 m^3/s). This indicates the importance of the regional flow in the study area and the contribution of the recharge to the aquifer located downstream of the subwatershed. Simulations using climate change scenario data predict an increase in the annual recharge from 2000 to 2100. This increase mainly occurs during the winter months and is caused by an increase in temperature and more frequent melt events. This increase in recharge is also observed in the baseflow. In order to assess the possible impact of land use change in the water cycle, combined with climate change, four land use scenarios were tested in the SWAT model. The changes in the future water balance were masked by the large changes induced by the climate change scenarios, and

thus land use change impacts were not considered with the coupled model. On average there will be more water available (recharge, stream flow, baseflow, groundwater elevation) in the subwatershed in winter and fall seasons. However, there will be changes in timing of water availability. Less water is predicated to be available during critical crop periods such as lower recharge and stream flow in spring and summer. This study has highlighted that a small subwatershed such as the LWC, with highly permeable soils, stresses on current water availability and dense agricultural activities, can be vulnerable to changes in the water budget for future conditions. It is important that predictive models are used to simulate water budgets, including future impacts of climate and land use change when possible, to ensure collective uses do not have adverse impacts.

TABLE OF CONTENTS

LIST OF FIGURES

LIST OF TABLES

1 INTRODUCTION

Around the world, groundwater is a critical resource for domestic use, industrial production and agricultural activities. For example, almost half of all drinking water worldwide comes from groundwater (Smith et al., 2016) and about 70% of the groundwater withdrawn is used for agriculture (Margat and van der Gun, 2013). In the province of Ontario (Canada), groundwater is used by approximately 30% of the total (urban and rural) population, although it is often the only available water source for rural supplies (Simpson, 2015). Thus, groundwater is an essential resource for agricultural production, including activities such as irrigation and livestock watering, and for potable supply using private wells.

When there is not enough water available in a given hydrosystem, various issues can occur surrounding competing uses. Water use conflict refers to the stresses regarding the water availability in an area or region given the current population and water usages (e.g. municipal supply, dewatering activities, agricultural use, ecosystems use) (Shifflett et al., 2014; Wolf, 1999). The approaches to examining water balance processes vary with scale (Barthel and Banhazf, 2016). For example, a major watershed water balance conducted using an integrated model may not capture the issues related to water use and conflict on a subcatchment scale, which could be relevant for supporting ecosystems. In southern Ontario, the increasing population in urban areas and surrounding smaller communities has created a higher pressure on water supply. Climate change has also added a level of uncertainty relating to future water supply plans (Etienne, 2014). The intensification of land use is straining aquifers due to the large groundwater demands (Wong, 2011). Small municipalities and townships have recently encountered difficulties initiating and maintaining water supply plans, especially in areas of water use conflict (Etienne, 2014).

Global changes from natural and anthropogenic sources (e.g. climate change, population growth, agricultural intensification) place great stress on water resources around the world (Cuthbert et al., 2019; Green et al., 2011; Taylor et al., 2013). Although projected future annual precipitation may not change much, intense rainfall events are expected to become more frequent. Warmer summer temperatures increased evaporation and more frequent extreme events could induce more intense dry periods with less water from runoff and low soil moisture (Bush and Lemmen, 2019; Expert Panel on Climate Change Adaptation, 2009; Larocque et al., 2019). In Ontario land uses have changed

significantly since 1950, with a marked intensification of agricultural activities where soils are most fertile and meteorological conditions are favourable. This has led to large areas of southern Ontario being intensively cultivated and dedicated to food production for the Great Lakes region (OMAFRA, 2019a). Agricultural practices have evolved to use soil water resources in a near-optimal way to ensure the highest productivity, while respecting current regulations. Nevertheless, farmers are now experiencing changing meteorological conditions that add increasing uncertainty to their productivity (Ray et al., 2019; Qian and Gameda, 2010).

The objective of this research was to examine future groundwater availability at the subcatchment scale for water-stressed areas dominated by agricultural use. This work considers potential future conditions that could be driven by a changing climate. The lower portion of the Whitemans Creek, a tributary of the Grand River watershed in southwestern Ontario, is presented as a typical case study. Much previous research has been done at the scale of the Grand River watershed. Notably, Wong (2011) conducted a water use inventory study, using data from the Ontario Permit to Take Water (PTTW) Database. Erler et al. (2019) used a fully integrated model to examine climate change impacts on the water resources in the Grand River watershed. For the entire Whitemans Creek subwatershed, Kovacs (2014) examined low water conditions and drought contingency planning. Starr and Levison (2014) used virtual water techniques to calculate regional water use from crop production. EarthFX (2018) completed a water budget and water quantity risk assessment for the Bright and Bethel well fields, using an integrated model encompassing the entire Whitemans Creek subwatershed and an area beyond. The current study differs from these previous studies in that the water budget of a small subcatchment, with intensive agricultural activity and large permitted water takings, is examined in a detailed manner in the context of land use changes and climate change, using newly collected field data and a coupled groundwater-surface water model.

This report summarizes the main scientific findings of the project funded by a joint research grant obtained by Marie Larocque, professor at UQAM, and Jana Levison, Associate Professor at University of Guelph, from the Innov'Action Agroalimentaire/Quebec-Ontario Cooperation for Agri-Food Research program sponsored by MAPAQ (*Ministère de l'Agriculture des Pêcheries et de l'Alimentation du Québec*; Quebec agriculture ministry) and by OMAFRA (*Ontario Ministry of Agriculture, Food and Rural Affairs*). More detailed results can be found in Aurélien (Ryan) Osman's Master's thesis (Osman, 2017) and in the published paper by Larocque et al. (2019).

2 STUDY AREA

2.1 General information

The Lower Whitemans Creek subcatchment study area (LWC; 63.55 km^2) is located in the lower portion of the Lower Whitemans Creek subwatershed (6th order stream; 404 km^2), a tributary of the Grand River watershed (6700 km^2) in southwestern Ontario (**Figure 1**). The LWC subcatchment is generally flat with elevations ranging from 360 to 254 m, and drains through Brant and Oxford Counties. This area is one of the most water-stressed in the region, having the highest demand for agricultural irrigation in the whole Grand River watershed (Wong, 2011). The population is mainly rural with the exception of the township of Burford with a population of 1,615 (Statistics Canada, 2017). All the residents in the LWC rely on private wells.

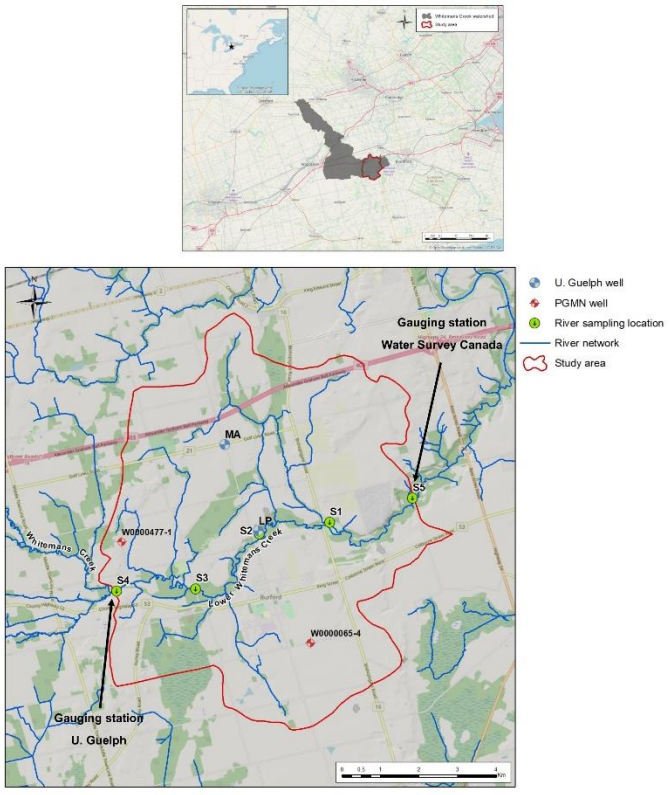

Figure 1. Location of a) the Lower Whitemans Creek in southwestern Ontario and b) the study site with instrumentation.

2.2 Geology

The surficial geology of the Whitemans Creek subcatchment is mainly composed of glacial sediments from the Late Wisconsin glaciation (**Figure 2**). The invasion by the Lake Ontario lobe (Ontario Geological Survey, 1981) has deposited sediments consisting primarily of outwash and glacio-lacustrine shallow-water deposits (AquaResources Inc., 2009). As the ice margin was retreating, large north-south trending ridges composed of sand and gravel transported by meltwater from the ice margin were deposited (Ontario Geological Survey, 1981).

After the ice retreated, lacustrine beaches and deltaic sediments formed a large deltaic and lacustrine complex. This complex known as the Norfolk Sand plain consist of medium to very fine sand and form the main surficial aquifer of the LWMC subwatershed (Ontario Geological Survey, 1981). Till deposits are present in the west (Port Stanley till) and in the east (Wentworth till). These deposits have lower hydraulic conductivity than the sediments of the Norfolk Sand plain (AquaResources Inc., 2009).

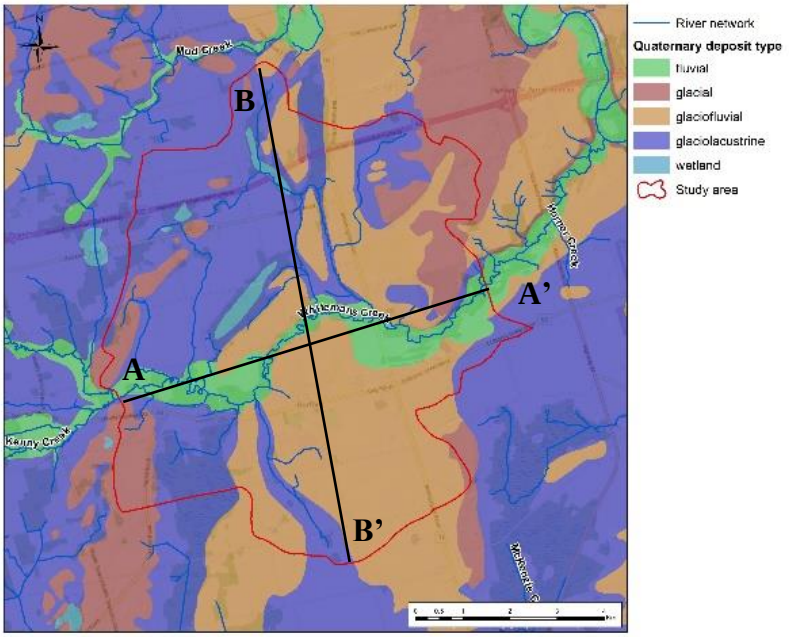

Figure 2. Surface deposits on the Lower Whitemans Creek (Ontario Geological Survey, 2010).

The stratigraphy of the study area is complex and composed of three aquifer layers and four aquitards. The two major aquifers are the outwash deposits of the Grand River formation which form the surficial aquifer and the Upper Erie Phase aquifer (Waterloo Moraine). These aquifers are separated by the Port Bruce till aquitard in most of the subcatchment except in the north-west part where both aquifers are connected. The bedrock is isolated from the sediments by the Lower Erie Phase aquitard for the entire study site.

The west-east cross section was taken from the inlet of the subwatershed to the outlet of the subwatershed (**Figure 3a**). The topography of the section analyzed is low relief, with an elevation ranging from 255 to 265 masl. Three main lithologies were identified in the overburden, gravel, sand, and clay. The documented limestone bedrock was reached at a depth of 220 masl. A top thin and uniform loam layer of approximately 1 m bgs is underlain by the shallow sand aquifer of a maximum thickness of 10 m in certain region. A gravel layer is also observed from the west to the center of the cross section between 250 to 235 masl. A 25-m thick clay layer between 245 to 220 masl underlies the sand layer. A silt pocket was identified at the well ID# 7187171 at the same depth as the clay layer. However, it is a possible that the silt pocket was misinterpreted and could have been clay. The limestone bedrock is located at 220 to 210 masl. It is noted that another pocket of silt is observed at the east part of the cross section.

The topography of the north-south cross section is low relief, with an elevation ranging from 260 to 245 masl (**Figure 3b**). The same lithologies of sand, gravel, and clay, as in the west-east cross-section were identified. The north-south cross section has fairly uniform lithology. A top thin and uniform loam layer at approximately 1 m bgs (below ground surface) is underlain by the shallow sand aquifer of a maximum thickness of 10 m in certain areas. A gravel layer is also observed from the west to the center of the cross section between 245 to 240 masl. A 25 m thick clay layer between 240 to 220 masl underlies the sand layer. The limestone bedrock is located at 220 to 210 masl.

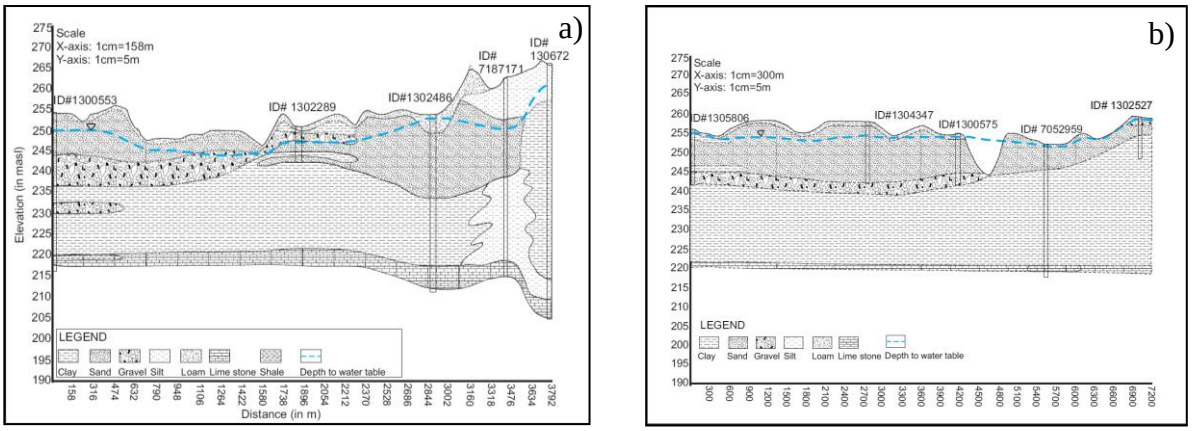

Figure 3. Geological cross-sections of the study area based on data from Government of Ontario (2017): a) east-west (A-A') and b) North-South (B-B') (Osman, 2017).

2.3 Hydrology and Hydrogeology

A Water Survey of Canada gauging station (02GB008; see **Figure 1** for location) has been recording flow rates at the outlet of the LWC since 1961. Daily flow rates vary between 0.12 and 82.90 m^3/s, with a median of 2.44 m^3/s. Annual flow rates vary between 2.08 and 7.18 m^3/s, with a median of 4.26 m^3/s.

Within the research site, two Provincial Groundwater Monitoring (PGMN) wells (W0000477-1 and W000065-4) wells are available with their borelogs and water level data (see **Figure 1** for location). A regional potentiometric map of the Quaternary sediments was built using 949 water level values from wells of the Water Well Information System (WWIS; MOECC, 2017). The wells were selected when stratigraphic information did not show any indication of a bedrock contact in order to have water levels from granular aquifers exclusively. Forcing points of 0 m depth were added along Whitemans Creek. Water levels were interpolated using the inverse distance weighting method. This resulted in the determination of an average water table depth of 6.9 m, with a maximum of 45 m. The deepest values are located in a small area in the eastern portion of the study site where the Whitemans Creek is deeply incised in the sediments while shallow groundwater levels are located in wetland areas in the western and central portion of the study site (**Figure 4**). The potentiometric map indicates that groundwater flows regionally from the West to the East towards the Grand River. Heads locally form several piezometric domes located at the boundary of the subwatershed to Whitemans Creek.

Groundwater is also flowing in and out of the study area, in particular along the southeast and south area. The largest hydraulic gradients are located along Whitemans Creek in the central and eastern portion of the area.

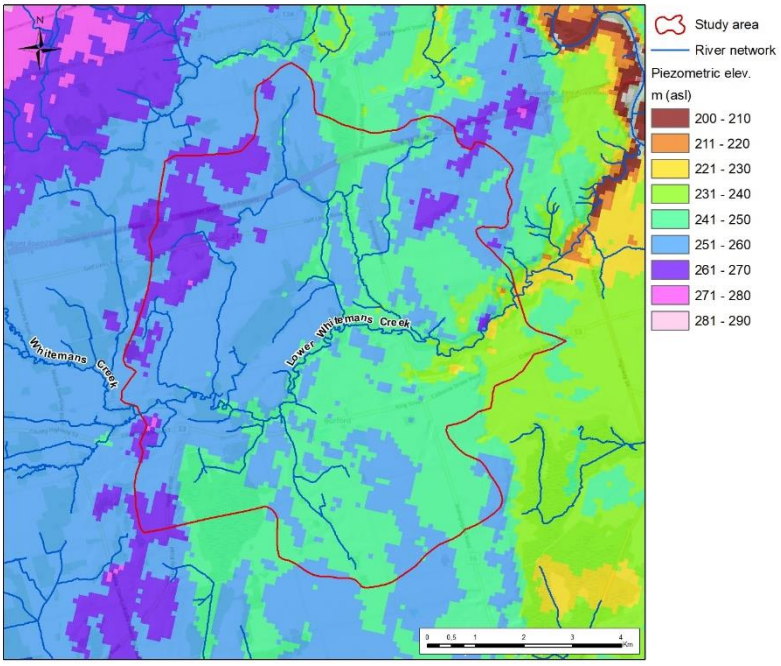

Figure 4. Potentiometric map for Lower Whitemans Creek.

2.4 Land use

The Whitemans Creek subwatershed has been almost exclusively dedicated to agricultural production for many decades (Wong, 2011). Aerial photographs were used to provide an estimate of the change in land use from 1960 to 1990 (photos dated 1964-1972-1980-1989) and annual crop inventories from Landsat photos were available since 2012 (Government of Canada, 2019). This information shows that land use has been almost constant since 1960, with 68-73% of the land dedicated to agricultural activities, 18-20% holding forest acreage, and 8-14% for urban use. The actual distribution and acreage of different crops between 1960 and 2010 was not documented in detail. It is assumed that the trends observed in the county for the main crops such as soybeans and tobacco could be used for the study area to estimate the historic land use. From 1950 to 1970, land uses were relatively constant with corn as the main cash crop and tobacco as the main specialty crop. Starting in the mid-1980s, tobacco production dropped greatly, replaced mostly by soybeans from thereon mostly cultivated in

2-year rotations with corn, and the main specialty crop has been ginseng. With the reduction of tobacco farming from 24% in 1950 to 2% in 2016 (OMAFRA 2019b; Government of Canada, 2019), and the increase in soybean acreage from 3 to 26% during the same period, the proportion of the area occupied by specialty crops has been reduced from 28 to 4% while that of cash crops has increased from 32 to 55%.

In recent years, corn and soybeans have been consistently the two main crops grown within the LWC subcatchment area (**Figure 5**). In 2016, these crops which were typically cultivated in a 2-year rotation at present, covered 50% of the subcatchment area (24 and 26% for corn and soybeans respectively; AAFC, 2018). In parts of the subcatchment, winter wheat is cultivated in rotation with corn and soybean, but this practice is marginal (3% of the area under winter wheat in 2016). The LWC has some of the largest specialty crops operations (including tobacco, ginseng and other vegetables) in southern Ontario, requiring regular irrigation (Shifflett et al., 2014). However, these specialty crops do not currently cover a large portion of the area (4% of the total area in 2016). In 2016, the proportion of land uses dedicated to urban activities, surface water, wetlands, trees and uncropped agricultural land are respectively 9%, 0.1%, 1%, 17% and 14% (AAFC, 2018).

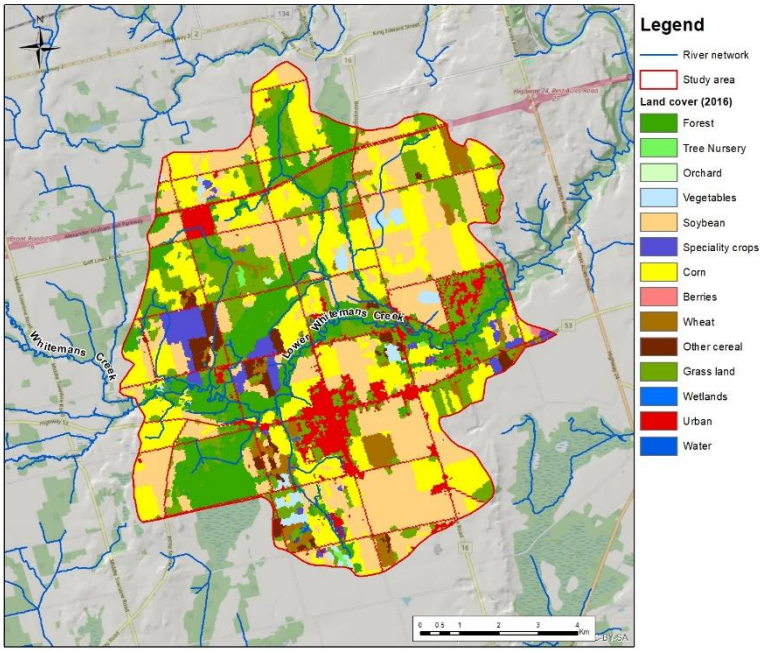

Figure 5. Spatial distribution of land use in 2016 (Canada Open Government, 2016).

2.5 Water use

In Ontario, permits to take water (PTTW) are required for water pumping (groundwater or surface water) exceeding 50 000 L/day. In 2014, the entire Whitemans Creek watershed had 125 PTTW, one of the Grand River subcatchments with highest numbers of PTTW (Shifflett et al., 2014). In 2016, the LWC had 47 active PTTW pumping the aquifer (12 permits), ponds (32 permits) and surface water (3 permits) for the equivalent of 182 mm/yr (MOECC, 2016). The PTTW program is currently undergoing a broad, rigorous review by the Ontario Ministry of the Environment, Conservation and Parks (MECP) motivated notably by public outcry around water bottling issues (Government of Ontario, 2019). In Ontario, the PTTW program is not an allocation of water, it is a permission to use water. Currently, permits are typically for 5 to 10 years and can be renewed. If permit holders let their permits lapse, they have to go through the current process, which includes conducting a detailed hydrogeological study (MOE, 2005). For surface water sources, a permit holder cannot take more than 20% of the 7Q20 flows (minimum 7 day flow with a return period of 20 years).

In the Whitemans Creek subwatershed, there have been various factors influencing the rate of PTTW applications/renewals. The permits increased slowly between the early 1960s to approximately 174 mm/yr in 1999. They peaked at 400 mm/yr in 2005 and decreased afterwards to 182 mm/yr in 2016 (**Figure 6**). The declared volumes of water use have increased from 3 mm/yr in 2006 (no declarations prior to 2005) to 18 mm/yr in 2012, and they fluctuate markedly from year to year. These values appear to be very small and are considered to underestimate the actual pumping rates.

In the LWC, water is used for irrigation, for drinking purposes and to feed animals. Irrigation is used in greenhouses, in the tree nursery, on sod, and on specific specialty crops (tobacco, ginseng, peas, beans and other vegetables). When using water need data estimated from FAO (2019), the total amount of irrigation needed for the specialty crops on the LWC is estimated to be approximately 14.2 mm/year. Although different from the declared pumped volumes, this value is of the same order of magnitude and thus seems realistic. The difference between the declared groundwater use and the estimated total groundwater use probably comes from uncertainties in the irrigation requirements of the crops. The township of Burford does not rely on a municipal water system and most houses have their own drinking water well. Considering the current population of 1615 in Burford (Statistics

Canada, 2016), and an average water use of 160 L/pers/day (Wong, 2011), groundwater pumped for drinking water purposes is estimated at 1.5 mm/yr. Water use to feed animals is estimated to be very low given the limited animal herds in the study area.

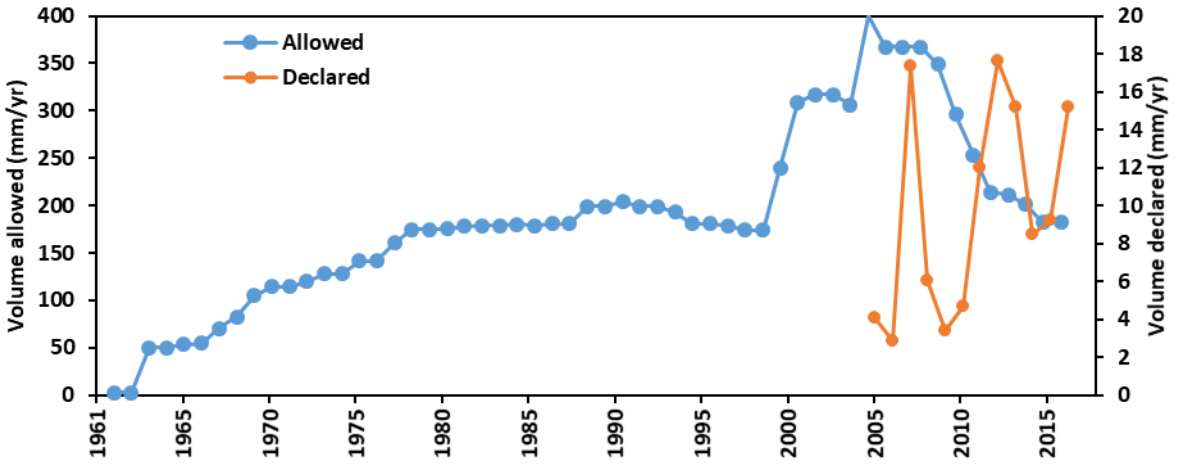

Figure 6. Evolution of volume allowed from the Permits to Take Water from 1961 to 2016, and declared water consumption from the aquifer from 2004 to 2016 (data from Ontario, 2016).

2.6 Past meteorological conditions

The meteorological data between 1961 and present was extracted from the ANUSPLIN interpolated data (10 km x 10 km grid; Government of Canada, 2017). During this period, the average annual precipitation varied between 515 and 1111 mm/y, with a median of 836 mm/y. The average annual temperature varied from 6.5 to 10.1°C, with a median of 7.7°C. Interestingly, both the total annual precipitation and the average annual temperature show a statistically significant increase (Mann-Kendall test, $p<0.01$). The maximum monthly temperature occurs in July (21°C average) and minimum in January (-6 °C average). Monthly precipitation increases throughout the year with higher precipitation in the fall months (**Figure 7**).

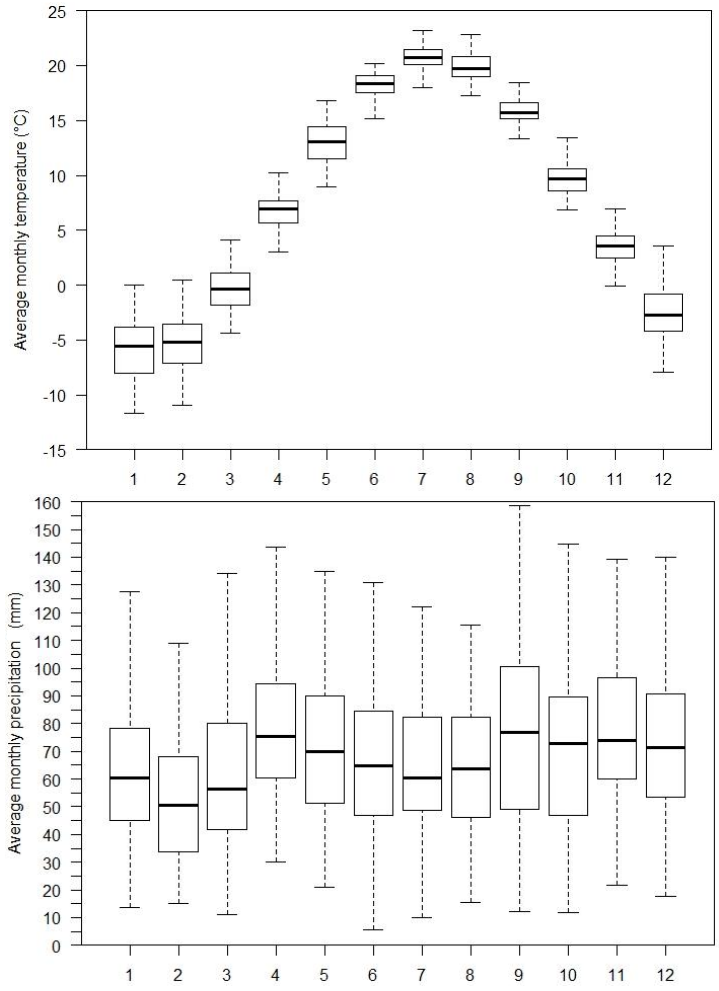

Figure 7. Average monthly temperature and average monthly precipitation (1960-2017).

The potential evapotranspiration calculated using the Oudin et al. (2005) method varies between 629 and 751 mm/year, with a median of 670 mm/year. The evapotranspiration has a statistically significant increase between 1961 and 2018 (Linear regression and ManKendall analysis, pvalue < 0.01).

3 METHODS

3.1 Site characterization

Characterization of the study area was conducted for the Master's thesis of Ryan Osman. Methods used for instrumentation, monitoring and field work are briefly overviewed here and details are available in Osman (2017).

3.1.1 Well drilling, sediment sampling and field testing

In April 2016, two new clusters of monitoring wells were installed in the subcatchment at 1) the Lion's Park, near Whitemans Creek and 2) at the intersection of Maple Avenue North (well MA) and Golf Links Road (well LP) (see **Figure 1** for location). The MA wells were drilled to depths of 7.6 and 15.2 m and the LP wells were drilled to depths of 3.5 and 7.6 m. They were completed with 50 mm diameter PVC pipe, with approximately 1.5 m screens at depth. The wells were equipped with *Solinst Leveloggers* to collect continuous water level data every hour, starting in May 2016. The water level data was corrected for atmospheric pressure using a *Solinst barologger* installed on site. The PGMN and GRCA wells data were provided by the GRCA.

Well cores were retrieved during drilling and analyzed to provide geological information. Sediments were sampled at different locations in the study area and were analyzed for granulometry in the laboratory. Infiltration tests and pumping tests were performed *in situ*. Details of the methods and results are in Osman (2017).

3.1.2 Flow rate measurements

The surface water flow rates were measured manually during each sampling round at five surface locations in the stream (see **Figure 1** for locations) using a velocity-area technique and a *Marsh McBirney Flo-Mate 2000 Flow meter*. Flow measurements were performed 13 times between November 2015 and October 2017. Manual measurements could not be performed during high flow periods such as the early spring and early winter (January to April 2016 and December 2016 to April 2017) because of safety concerns.

A stream gauging station was installed at the inlet of the subcatchment in January 2016 (see **Figure** 1 for location). The stream gauging station was instrumented with a *Solinst level logger* to continuously measure the stage at the inlet of the subcatchment between January 2016 and August 2017 (see Osman, 2017 for details). The cross-section at the location of the gauging station was such that the floodplain is often occupied by the stream during the high-water season. Two distinct rating curves would have been necessary to represent these conditions but these could not be obtained due to unsafe conditions to measure flow rates during high flow periods when the water exceeds the low flow cross section. For this reason, the continuous flow rates estimated at this station were not used in the numerical modelling.

3.1.3 Water sampling

Water sample analysis was carried out monthly over the study period for stable isotopes of water, electrical conductivity, and ^{222}Rn, a tracer of groundwater flow to surface water. This was conducted in order to better understand groundwater-surface water interactions between the aquifer and Whitemans creek. Please refer to Osman (2017) for detailed information about the associated methods and results of the water sampling analyses.

3.1.4 Quantification of the growing season and growing degree days

The length of the growing season is critical to understand how this variable has evolved through time and how it could be impacted by climate change. The method used here is the one suggested by AAFC (2018). It is calculated in days starting from the seeding date, 10 days after the average daily temperature is above 5^{o}C, and ending at the first fall frost when the minimum daily temperature reaches 0^{o}C (or until October 31st). Growing degree days are computed by summing the number of degrees Celsius above the reference temperature of 10°C.

3.2 Flow modelling

3.2.1 Surface flow simulation with SWAT

A SWAT model (Arnold et al., 2012) was developed for the study area. The model was constructed using the Arc-SWAT interface to define the hydrologic response units (HRU). HRU's are

simplifications of three different surface layers: slope (Digital Elevation Model – DEM), land use (from LANDSAT data) and soil (from the integrated Canadian soil database). The SWAT soil database was used to define soil properties such as porosity, saturated hydraulic conductivity, soil water retention curves, etc. The combination of the three layers resulted in 2825 HRUs with areas between 400 m^2 and 1.3 km^2. Land use for each HRUs was determined based on the data from AAFC (2018). The stream network was also built with the Arc-SWAT interface. Daily precipitation and temperature data from the ANUSPLIN interpolated grid dataset (Government of Canada, 2017) were used as input to the model, and considered homogeneous over the entire study area.

Because the LWC subwatershed is not a headwater catchment (there is an inflow of water from the upstream portion of Whitemans Creek), surface water inflow at its upstream boundary was needed. For calibration purposes, a simple inlet-outlet flow rate relationship was established using the brief period during which flow rates were measured at the inlet. These values were used in the SWAT calibration. However, due to the absence of a long-term upstream gauging station at the LWC inlet, it was necessary to predict inflows to the study area for future simulations. To do this, the simple lumped conceptual MOHYSE hydrological model (Fortin and Turcotte, 2007) was calibrated using flow rate time series at the outlet between 1961 and 2016. The model represents relatively well total flow rates at the outlet (Nash-Sutcliff coefficient of 0.33), potential and actual evapotranspiration, as well as snow accumulation and melting. The calibrated parameters in MOHYSE are thus used to represent inflows at the upstream boundary of the study area for past and future conditions.

The SWAT model was calibrated using the automatic calibration procedure built in SWAT (SWAT-CUP) to reproduce flow rates measured at the outlet gauging station between 1961 and 2016. Following the work of Arnold et al. (2012), 20 parameters were selected to be modified during the automated process to minimize the Nash-Sutcliff coefficient. These parameters are related to runoff, baseflow and snow melt in the model. The results indicate that the model is sensitive to four of these parameters (**Table 1**). **Figure 8** illustrates the simulated stream flow at the outlet of the watershed compared to the measured values at the gauging station. The mean error is 0.1 m^3/s, the mean absolute error 0.64 m^3/s, and the RMSE is 1.17 m^3/s.

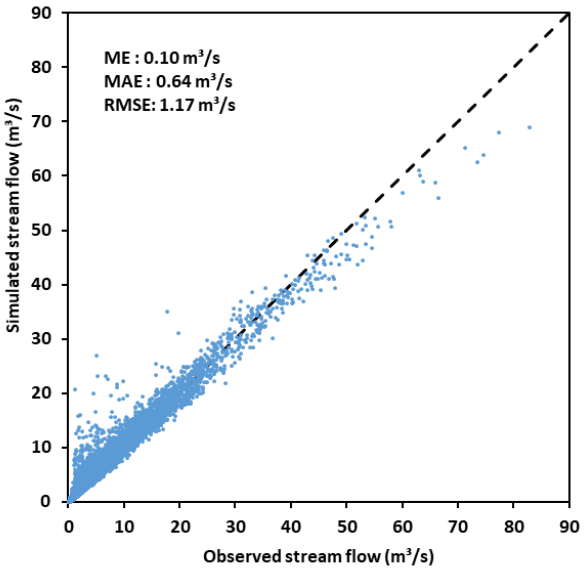

Figure 8. Simulated stream flow from SWAT compared to the observed stream flow at the outlet gauging station.

Table 1. Calibrated parameters for the SWAT model.

Parameter	Description	Value
CN2 (-)*	Initial RCN2 : relative change	-0.11
ALPHA_BF (-)*	Baseflow alpha factor	0.89
GW_DELAY (days)*	Groundwater delay time	4.79
GWQMN (mm)*	Threshold depth of water in shallow aquifer	1221
SFTMP (^{o}C)	Snowfall temperature	1.03
SMTMP (^{o}C)	Snowmelt base temperature	-1.65
SMFMN (-)	Melt factor for snow on Dec 21	2.27
ESCO (-)	Soil evaporation compensation factor	0.54
EPCO (-)	Plant uptake compensation factor	0.73
GW_REVAP (-)	Groundwater revap coefficient	0.04
SOL_AWC (-)	Avail water capacity of soil layer: relative change	-0.12
SURLAG (-)	Surface runoff lag coefficient	8.62
SMFMX (-)	Melt factor for snow on June 21	3.91
RCHRG_DP (-)	Deep aquifer percolation factor	0.05
REVAPMN (-)	Threshold depth of water in shallow aquifer for revap conditions	131
OV_N (-)	Manning n value for overland flow: relative change	0.18
TIMP (-)	Snowpack temperature lag factor: relative change	-0.37

*Most sensitive parameters

3.2.2 Groundwater flow simulation with MODFLOW

A 3D groundwater flow model was developed in MODFLOW-2005 with the Groundwater Modeling System interface (Harbaugh, 2005). The model covers the entire study area and extends vertically to incorporate the sediments and the bedrock formation. It consists of a 20 m x 20 m grid with 457 columns and 540 rows. The top layer of the model was interpolated from the 20 m resolution surface topography DEM from Canada Open Data (Canada 2017). Vertically, the model is composed of seven layers, each representing a stratigraphic unit. The elevations and spatial distribution of these layers were interpolated using data from the Ontario Ministry of Energy, Northern Development and Mines database of 3D Quaternary model (MENDM, 2017). **Figure 9** illustrates a West-East cross-section of the MODFLOW model. The second geologic unit (Port Bruce Till-ATB1) was separated into three numerical layers to minimize the effect of the strong hydraulic conductivity difference between this aquitard and the two major aquifers. During the calibration process of the transient model, a second hydraulic conductivity unit was added to the surficial aquifer in the area of well W065 to ensure proper calibration. This hydraulic conductivity zone corresponds to the area covered by the glaciofluvial deposits (see **Figure 2**).

The potentiometric map of the study area was used to impose the general head boundary values at the West and East boundaries (North and South limits were set as no flow boundaries). The base of the model was set as a no flow boundary and a recharge condition was applied at the top of the model. The average recharge estimated using the SWAT model was used as a spatially constant value in the steady-state MODFLOW model. In the transient-state simulation, the average monthly recharge from the calibrated SWAT model was used and kept constant spatially. The various small streams in the study area were represented using the Drain package. Whitemans Creek was represented using the River package to allow the possibility for the creek to recharge the aquifer. The conductance value for the small streams represented with Drains was set to a high value (10 $m^2/m/d$). For Whitemans Creek (River package) the conductance was set to a lower value (1 $m^2/m/d$) since the creek flows on alluvial sediments that have lower hydraulic conductivities. Drain and River elevations were set to 2 m below the surface.

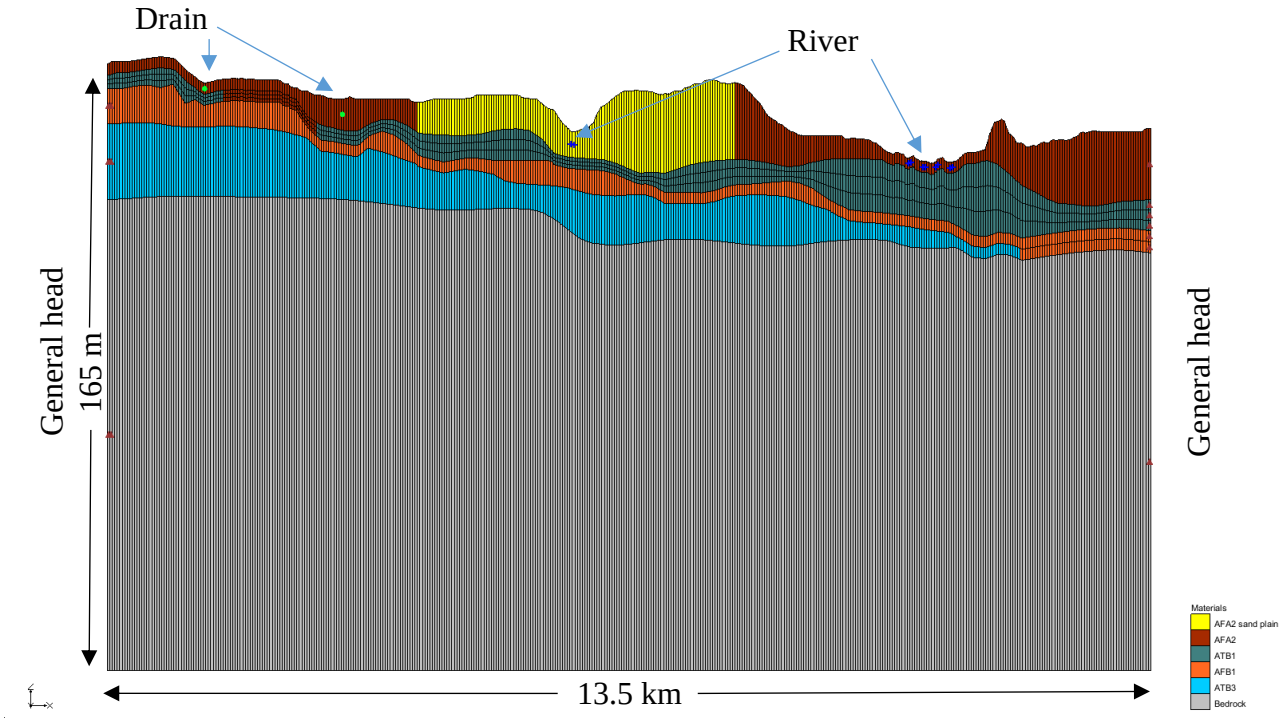

Figure 9. West-East cross section of the MODFLOW model. Total thickness is 165 m and total length of the cross-section is 13.5 km.

The MODFLOW model was calibrated in steady-state using the automatic calibration procedure in PEST (Doherty and Hunt 2010) to reproduce available the 597 head data from MOECC (2017), from the two PGMN wells, and from the MA and LP wells. Seven parameters (

Table 2) were calibrated to minimize the RMSE.

Table 2. Parameter intervals and calibrated values for the MODFLOW model. The numbers in parentheses are the specific yield values (S_y).

Parameter	Interval	Calibrated value
AFA2 sand plain: Kh (S_y)	1-100 m/d (0.1-0.2)	14 m/d (0.17)
AFA2:Kh (S_y)	1-100 m/d (0.1-0.2)	12 m/d (0.15)
ATB1: Kh (S_y)	$5x10^{-4}$-$5x10^{-3}$ m/d (0.005-0.05)	0.01 m/d (0.02)
AFB1 : Kh (S_y)	1-100 m/d (0.1-0.2)	20 m/d (0.15)
ATB3 : Kh (S_y)	$5x10^{-4}$-$5x10^{-3}$ m/d (0.005-0.05)	0.003 m/d (0.02)
Bedrock : Kh (S_y)	0.01-0.1 m/d (0.01-0.1)	0.056 m/d (0.06)

The most sensitive parameters are the recharge and the hydraulic conductivity of the surficial aquifer (AFA2). The MODFLOW model was then calibrated manually (trial-and-error procedure) in transient state, using monthly stress periods, to determine the values of the storage coefficient for the study area. The calibration statistics for the steady state model were: mean error 0.7 m; mean absolute error 2.58 m; and RMSE 3.91m. For the transient model, the mean error was 0.15 m, the mean absolute error 0.37 m and the RMSE 0.5 m (**Figure 10**). The calibrated simulated transient water levels are close to the observed heads and they follow the variation in time and amplitude closely (**Figure 11**). Note that only the results from the two PGMN wells are shown because they have long time series.

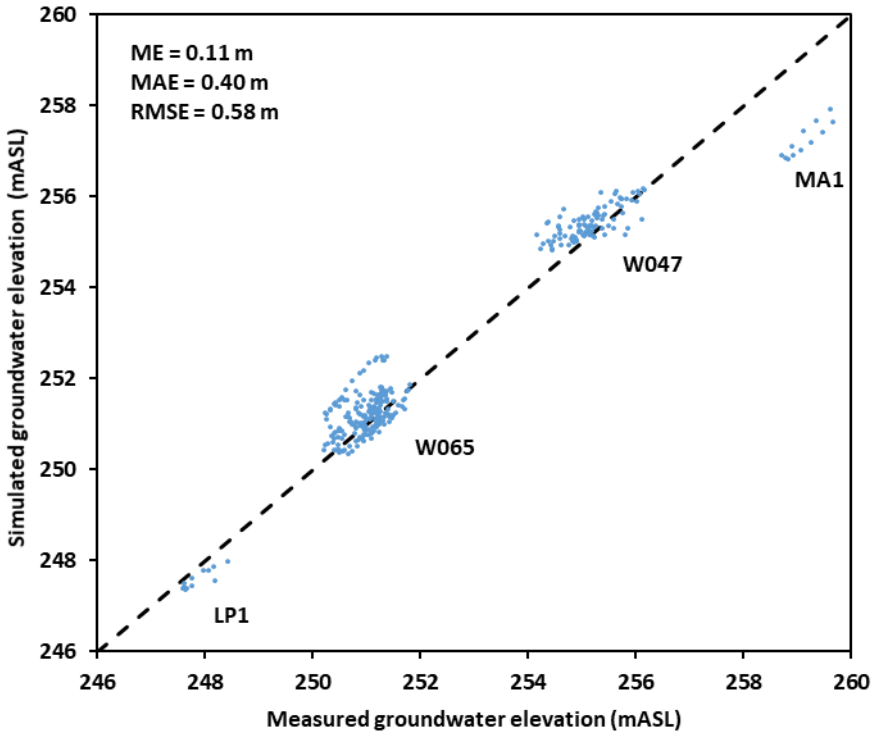

Figure 10. Observed and calibrated groundwater levels for the transient MODFLOW model.

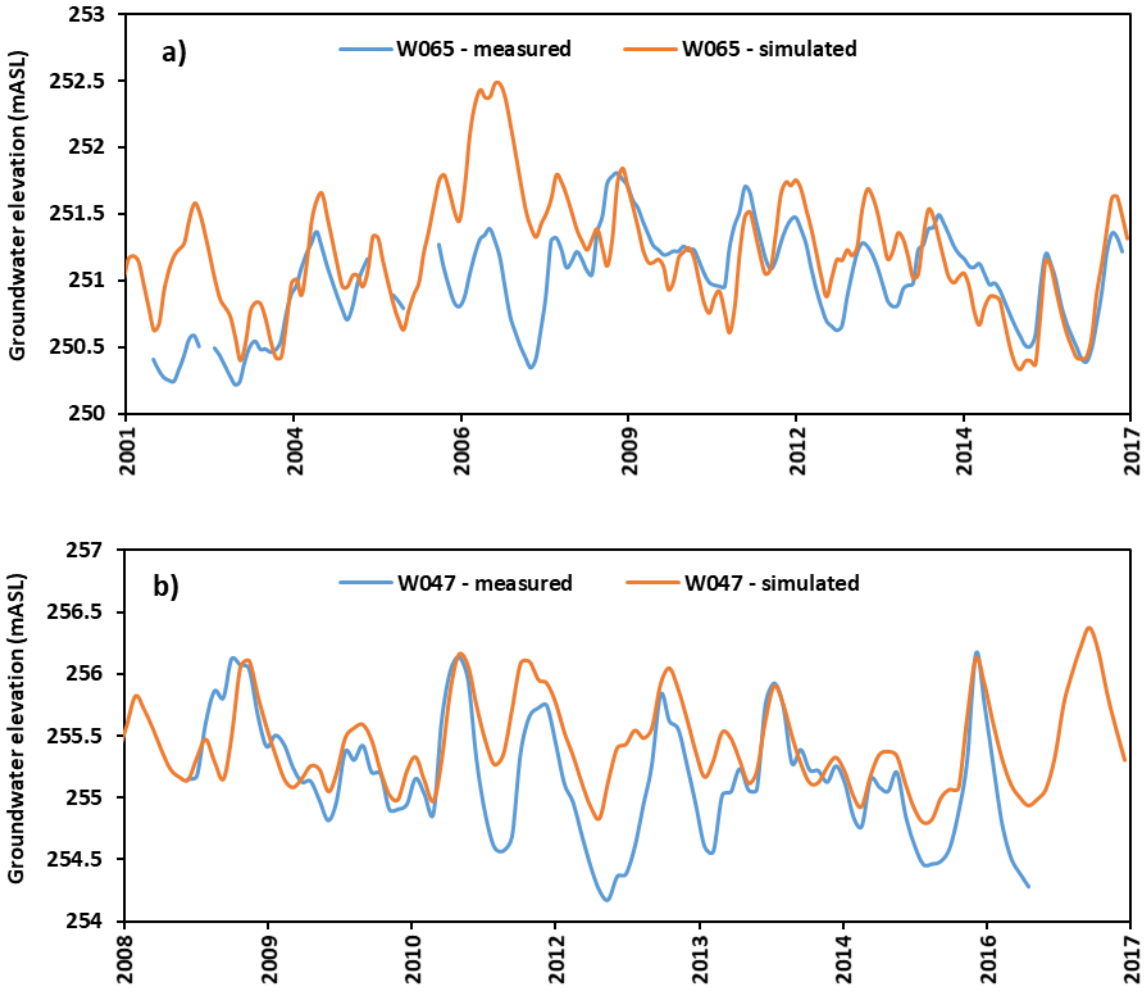

Figure 11. Observed and simulated heads a) for well W065 and b) for well W047.

3.2.3 Integrated surface water and groundwater flow simulation with SWAT-MODFLOW

The SWAT-MODFLOW (version 3) model (Kim et al., 2008) was used to simulate integrated surface water and groundwater flow. The calibrated SWAT model was used to represent all surface flows, and the calibrated MODFLOW model was used to represent groundwater flow. In the coupling process, the SWAT model was run using a daily time step while the MODFLOW was run using a monthly time step. In this way, the monthly recharge from SWAT was transferred to the MODFLOW module at the end of each month. Similarly, groundwater discharge to streams and water table elevation were distributed equally to the next 30 days into the SWAT module. The coupled model

was not recalibrated. The coupled model was run between 1961 and 2017 to reproduce past conditions. For the climate change scenarios, the coupled model was run for three different time windows (1990-2010, 2030-2050, 2070-2090) with 5 years of warm up. This was done to reduce computing time and output data size.

3.3 Future scenarios

3.3.1 Climate change

Climate change scenarios were provided by the Ouranos Consortium. The scenarios are derived from two Representative Concentration Pathways, RCP4.5 and RCP8.5. The RCPs describe potential futures of the main drivers of climate change, including greenhouse gas and air pollutant emissions. The scenarios are named based on the change in radiative forcing in 2100 compared to pre-industrial values. The RCP4.5 scenario (optimistic) represents an increase in radiative forcing of 4.5 W/m^2 relative to pre-industrial values. It is associated with a capping of emissions which would stabilize the radiative forcing caused by climate change in 2100. The RCP8.5 scenario (pessimistic) represents no change in current human behaviour. Emissions continue to rise beyond 2100 when the radiative forcing is increased by 8.5 W/m^2 relative to pre-industrial values. Ten climate simulations were selected by Ouranos using a cluster analysis based on the change in temperature and precipitation between the periods of 1971-2000 and 2031-2060. Using this methodology, 22 simulations were selected out of the 54 available at the time (11 for each of the two RCP scenarios; **Table 3**). In an effort to reduce the number of simulations, a second selection step was done to choose one scenario close to the 25^{th}, 50^{th} (median) and 75^{th} percentiles for temperatures. These scenarios represent a wide range of trends in seasonal temperature and precipitation (**Figure 12**). The coolest scenario (hereafter named scenario 1; INM-CM4_RCP45) is a little cooler in 2100 than the 25^{th} percentile of all scenarios. The average scenario (hereafter named scenario 2; NorESM1_RCP45) is a little cooler in 2100 than the ensemble mean. The warmer scenario (hereafter named scenario 3; CMCC-CMS_RCP85) is close to the 75^{th} percentile of all scenarios. The temperature increases throughout the simulation period, starting around 2000. Precipitation changes do not show any significant trends, but year-to-year variations are higher after 2000.

Table 3. Models and scenarios used in the study.

No.	Modeling Center	Model	RCP	Member
1	INM	INM_CM4	4.5	r1i1p1
1a	INM	INM_CM4	8.5	r1i1p1
2	NOAA_GFDL	GFDL_ESM2M	4.5	r1i1p1
2a	NOAA_GFDL	GFDL_ESM2M	8.5	r1i1p1
3	MPI_M-	MPI_ESM_LR	8.5	r1i1p1
3a	MPI_M	MPI_ESM_LR	4.5	r1i1p1
4	CCCMA	CanESM2	8.5	r1i1p1
4a	CCCMA	CanESM2	4.5	r1i1p1
5	CSIRO	BOM-ACCESS1_3	4.5	r1i1p1
5a	CSIRO	BOM-ACCESS1_3	4.5	r1i1p1
6	BNU-	BNU_ESM	8.5	r1i1p1
6a	BNU	BNU_ESM	4.5	r1i1p1
7	MOHC	HadGEM2_CC	8.5	r1i1p1
7a	MOHC	HadGEM2_CC	4.5	r1i1p1
8	NCC	NorESM1	8.5	r1i1p1
8a	NCC	NorESM1	4.5	r1i1p1
9	IPSL	IPSL_CM5B_LR	4.5	r1i1p1
9a	IPSL	IPSL_CM5B_LR	8.5	r1i1p1
10	CMCC	CMCC_CMS	8.5	r1i1p1
10a	CMCC	CMCC_CMS	4.5	r1i1p1
11	IPSL	IPSL_CM5A_LR	8.5	r1i1p1
11a	IPSL	IPSL_CM5A_LR	4.5	r1i1p1

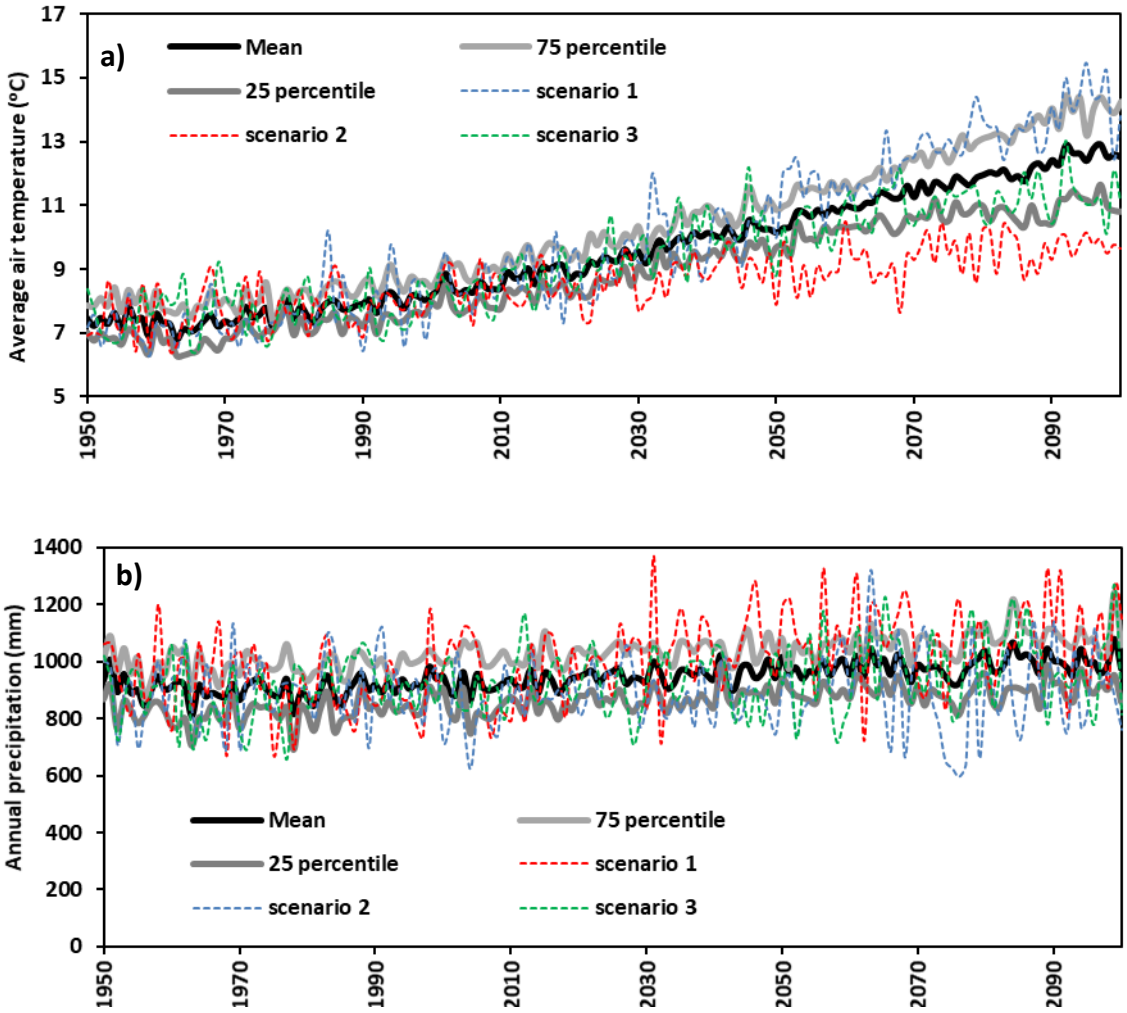

Figure 12. Ensemble mean, 25th and 75th percentiles of the climate change scenarios, with the three selected scenarios with a) average temperature and b) annual precipitation.

3.3.2 Land use change scenarios

The land use scenarios were developed for 1951-1970, 2071-1990, 1991-2011 based on the past land use conditions using OMAFRA database (OMAFRA, 2019b) and the rasters were developed from 2012 to 2016 using AAFC database. Four future land use scenarios were used, with changes starting in 2017 (**Table 4**). First, a business as usual scenario is used where 2016 land uses are maintained until 2100 (50% of the area under corn-soybean rotation, 3% under corn-soybean-winter wheat/green manure rotation, and 14% of uncropped agricultural land). The second scenario represents lower

water use that could be the result of warmer and dryer conditions where cash crops would become less productive, and the uncropped agricultural land represents 36% of the study area (more than twice that of 2016) while the combined corn and soybean acreages are reduced to 28% of the area. The third scenario is meant to test the hydrological impact of implementing best management practices aimed at reducing soil erosion, nutrient loss, and crop resilience (Gaudin et al., 2015). In this scenario, all the parcels under the corn-soybean rotation are transformed to a corn-soybean-winter wheat/green manure rotation. In this scenario, winter wheat covers 18% of the area on average over the 3-year rotation while the combined corn and soybean acreages are reduced to 36% on average. The fourth scenario is used to represent an increase in corn and soybean acreages that could result in increased water use as the climate becomes warmer and dryer. In this scenario, all the uncropped agricultural land is converted to corn and soybeans (2-year rotation) which thereon covers 64% of the study area.

Table 4. Land use change scenarios.

Scenario	Crops
1. Business as usual	Same as in 2016
2. Lower water use	• 100% increase in uncropped agricultural land. • This increased uncropped area from corn and soybean areas. • Corn-soybean crops switched every year. • All other land uses kept constant.
3. BMP scenario	• All parcels under corn-soybean rotation transformed to corn-soybean-winter wheat/green manure rotation. • Corn, soybean and winter wheat/green manure alternated throughout the simulation (3-year rotation). • All other land uses kept constant.
4. Higher water use	• Corn and soybean acreages were increased from 50 to 64% of the study area. • All the uncropped agricultural land converted to the corn-soybean rotation. • All other land uses kept constant.

Note: all land use changes were started in 2017 and kept constant until 2100.

4 RESULTS

4.1 Past and current conditions

Detailed results of the field study are available in Osman (2017). Some key results are presented herein.

4.1.1 Groundwater recharge

The average annual baseflows estimated with the Lyne and Hollick (1973) method vary between 1.09 and 4.02 m^3/s with an interannual median of 2.36 m^3/s (**Figure 13**). This means that, on average, 55% of the median flow rate at the outlet comes from the aquifer. Because the gauging station is located at the outlet of the Whitemans Creek, the estimated baseflow is an average over the entire watershed. If geology was homogeneous over the entire Whitemans Creek watershed, the baseflow coming from the study area would be proportional to its relative area (63.55/385 = 17%). However, a portion of the Whitemans Creek watershed has low permeability sediments. The proportion of the study area on the total permeable area of the Whitemans Creek is estimated to be approximately 31% (63.55 km^2/208 km^2). Using this proportion, baseflow from the study area varies between 0.34 and 1.25 m^3/s with a median of 0.73 m^3/s, which corresponds to 159 and 585 mm/yr and an interannual median of 344 mm/yr. AquaResource Inc. (2009) reported recharge over the entire LWC area to be "higher than 350 mm/yr".

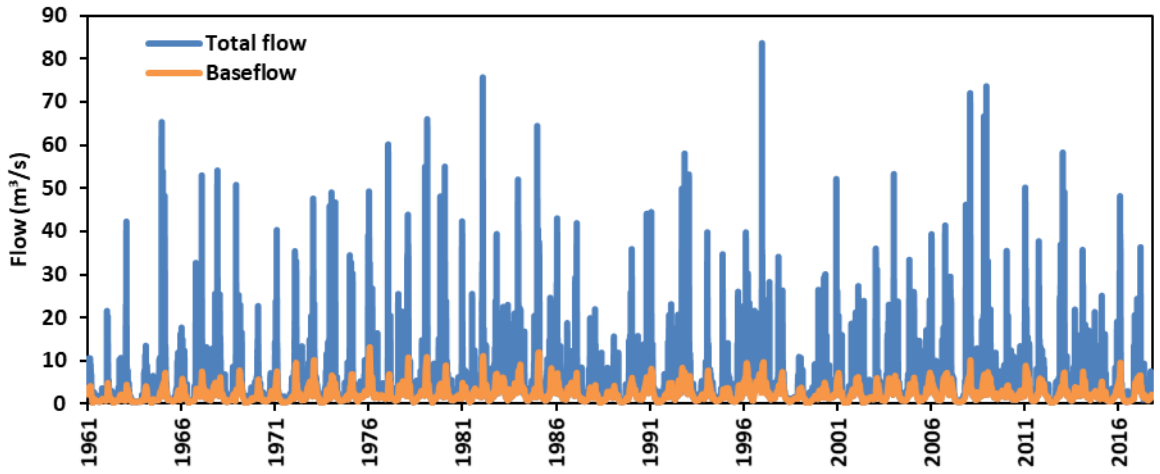

Figure 13. Daily total flow rates and base flows.

Because runoff is limited over the study area, the increase in flow rates between the inlet and the outlet of the study area can be attributed to recharge which flows to the river as baseflow. This contribution was estimated using the difference between flow rates near the outlet and flow rates at the upstream gauging station, measured manually 11 times between November 2015 and October 2017 (two measurements were excluded: one because the measured flow rate on May 2016 at the inlet was underestimated and one because the manually measured flow rate on September 2017 at the outlet was underestimated). The results show that during these measurements, the average increase in flow rates was 0.31 m^3/s, which is equivalent to 148 mm/yr over the study area (**Figure 14**). This value is close the lowest baseflow estimated with the Lyne and Hollick (1973) baseflow separation method. Baseflow values were estimated by direct measurements of total flow differential for a maximum total flow rate at the outlet of 2.25 m^3/s which is close to the median outflow rate, but much lower than the maximum measured outflow rate of 82.90 m^3/s between 1961 and 2017. If flow gradients had been measured during floods, it is probable that baseflow would also have been higher (**Figure 14** hints at the fact that baseflows tend to increase with flow rates).

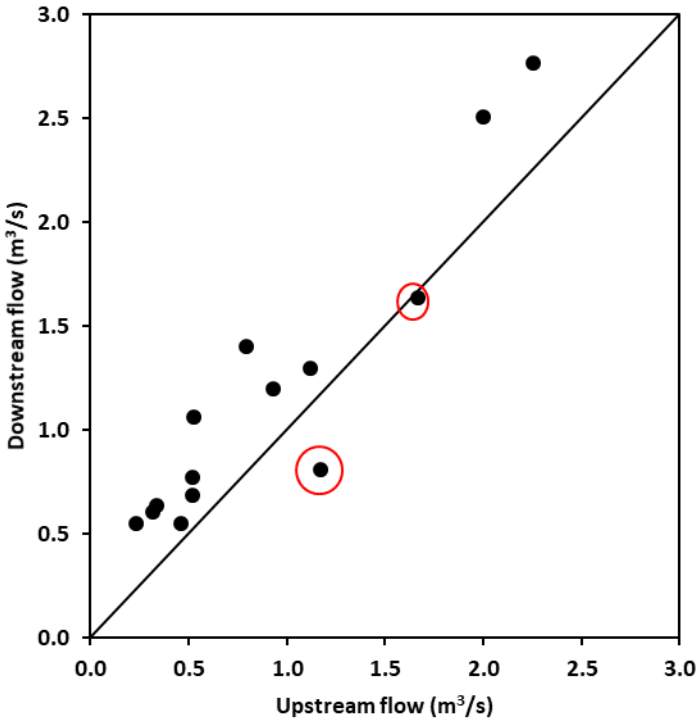

Figure 14. Downstream flow rate as a function of the upstream flow rate on the study area.

4.1.2 Growing season characteristics

Between 1961 and 2017, the growing season varied between 151 and 229 days, with a median value of 184 days with a longer growing season of 26 days that is statistically significant (Mann-Kendall, $p<0.05$) (**Figure** 15**a**). The median start of the growing season was Julian day 106 and has varied between March 14 (2012) and April 29 (1965). There has been a statistically significant change to an earlier start of the growing season (Mann-Kendall, $p<0.05$). Precipitation during the growing season varied between 234 mm (1964) and 680 mm (2000), with a median value of 412 mm and no statistically significant change through time. Temperature during the growing season varied between 14.7ºC and 17.7ºC, with a median value of 16.4ºC and a statistically significant (Mann-Kendall, $p<0.01$) increase between 1961 and 2017 (Mann-Kendall, $p<0.01$). PET during the growing season varied between 515 and 683 mm, with a median value of 593 mm and a statistically significant increase between 1961 and 2017 (Mann-Kendall $p<0.01$). The growing degree-days between 1961 and 2017 varied between 1820 and 2483 with a median value of 2129 degree days (**Figure 15b**). Given the increase in the length of the growing season, it is not surprising that the degree-days show a statistically significant increase between 1961 and 2017 (Mann-Kendall, $p<0.01$). These values are similar to the baseline values estimated for southern Ontario, having growing degree-day values higher than 1800 days for the 1971-2000 period (AAFC, 2018).

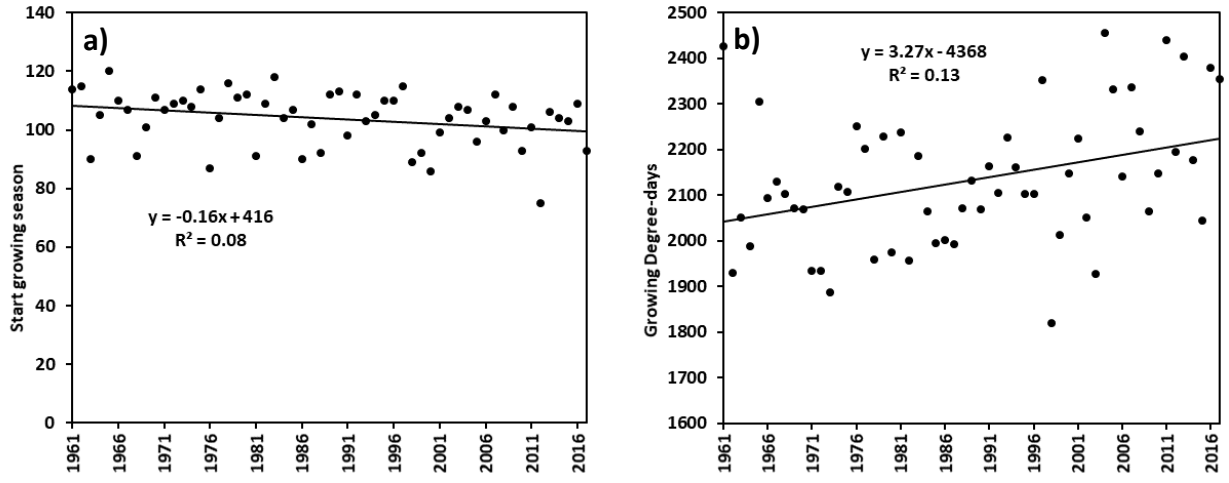

Figure 15. For the study area between 1961 and 2017 a) start of the growing season and b) growing degree days.

4.1.3 Net precipitation and actual evapotranspiration

Net annual precipitation (P-PET) varies between -137 and 459 mm/yr, with a median of 165 mm/yr (**Figure 16**). Drought years where net precipitation is negative occurred in 1963, 1971, 1998, 2007 and 2012. The warmest years occurred in the last two decades with maximum annual average temperatures of 10°C, 9.3 °C, 10.1 °C, and 9.5 °C in 1998, 2002, 2006 and 2016 respectively.

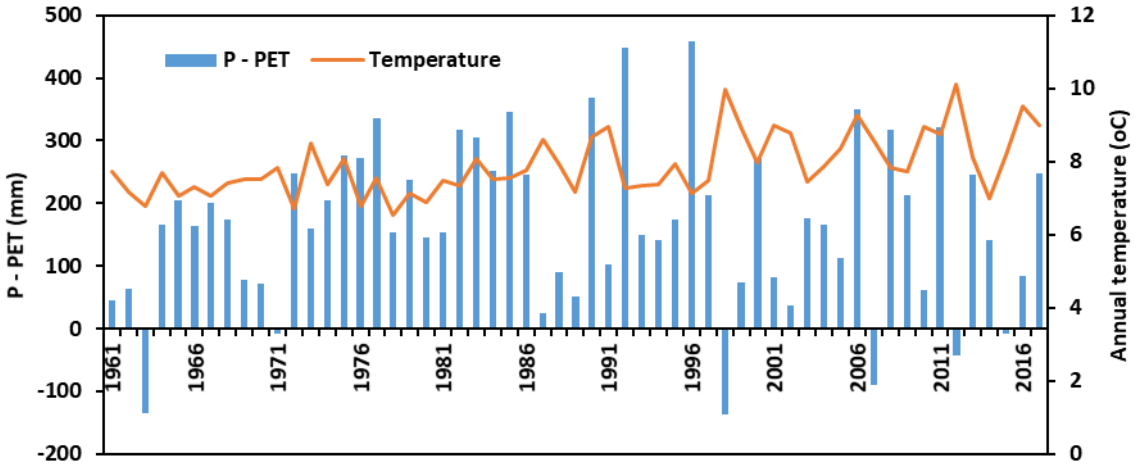

Figure 16. Net annual precipitation (P - PET) and average annual temperature between 1960 and 2018.

Actual evapotranspiration (precipitation minus flowrate at the outlet) varied between 313 and 654 mm/yr (average 502 mm/yr; data not illustrated here). These values are relatively high and apparently indicate that the evapotranspiration demand is satisfied to the level of 74% (AET/PET).

The available water in excess of the potential evapotranspiration during the growing season is zero most of the time (median value -164 mm), except during very wet years where the growing season precipitation was exceptionally high, such as in 2000 (680 mm). This means that there is almost never infiltration and recharge of the aquifer during the summer period. During this period, baseflow to the river is most probably driven by the slow decrease of groundwater levels in the sand aquifer which has been replenished during the spring snowmelt period.

4.1.4 Water budget

A complete water budget cannot be easily calculated for the study area because of the high uncertainty with all the estimated flows. Nevertheless, **Figure 17** allows the comparison of the different terms of the water budget and estimation of their variability (or uncertainty).

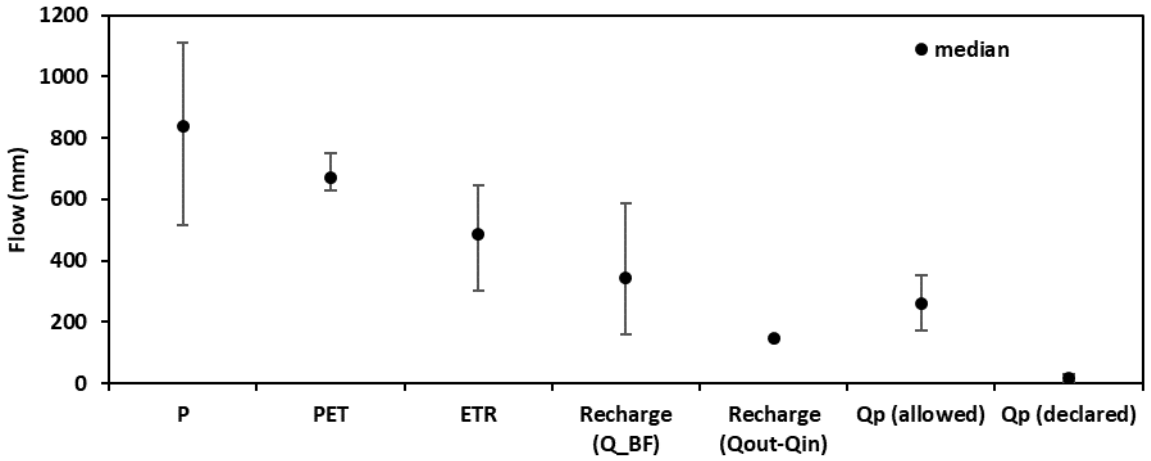

Figure 17. Components of the water budget. P, PET, AET and recharge estimated with baseflows are for 1961-2017. Recharge estimated with the difference in low flows is for the year 2017. Allowed (permitted) groundwater pumping values are from 1962 to 2016 while declared groundwater pumping values are for the 2005 to 2016 period. Error bars indicate minimum and maximum values.

Potential evapotranspiration is not much higher on average than actual evapotranspiration (667 mm compared to 502 mm). In warm years, net precipitation that is available for groundwater recharge and runoff can be very low. Recharge estimated with the difference between outflow and inflow is similar to the mean recharge estimated from baseflow separation (344 mm compared to 148 mm). Declared groundwater pumping is very small compared to all the other flows. However, the average permitted groundwater pumping rate (259 mm) is of a magnitude similar to that of the average recharge. This is an indication that if pumping was to increase significantly in response to dryer conditions, the LWC could be at high risk of drying out during low flow periods.

4.2 Future conditions from climate change scenarios

In this work, the reference period used for comparison is defined as 1971-2000 and two future periods are defined, 2031-2060 and 2071-2100 (**Table 5**). Comparing observed meteorological variables with

those simulated with the three selected scenarios for the reference period shows that the simulated scenarios have more precipitation on average than the observed values (between 21 mm for scenario 3 and 35 mm for scenario 1).

Table 5. Comparison of reference values (1971-2000) with future conditions (2031-2060 and 2071-2100) for annual precipitation, temperature, PET and net precipitation (P-PET).

Scenario	Period	P (mm/yr)	T (°C)	PET (mm/yr)	P-PET (mm/yr)
Observed	**1971-2000**	874	7.7	671	203
Scenario 1	**1971-2000**	909	7.8	673	236
Scenario 2	**1971-2000**	905	7.7	670	234
Scenario 3	**1971-2000**	895	7.7	671	224
Scenario 1	**2031-2060**	882 (-27)[1]	9.0 (+1.2)	707 (+34)	175 (-61)
Scenario 2	**2031-2060**	928 (+23)	10.1 (+2.3)	764 (+94)	165 (-69)
Scenario 3	**2031-2060**	1073 (+178)	10.7 (+3.0)	779 (+108)	294 (+70)
Scenario 1	**2071-2100**	872 (-37)	9.7 (+1.9)	734 (+61)	138 (-98)
Scenario 2	**2071-2100**	985 (+80)	11.2 (+3.5)	807 (+137)	179 (-55)
Scenario 3	**2071-2100**	1069 (+174)	13.6 (+5.9)	898 (+227)	171 (-53)

[1] Values in parentheses are changes between future periods (2031-2060 and 2071-2100) and the reference period (1971-2000)

Average temperatures, and consequently PET, are very similar to the observed values for the three scenarios. Because P is overestimated, the simulated P-PET for the reference period is also larger (between 21 mm for scenario 3 and 33 mm for scenario 1). Although they were bias-corrected for the 1971-2000 period, the simulated past meteorological conditions do not perfectly fit the meteorological observations.

The future precipitation simulated with the three scenarios are similar to those of the reference period for scenarios 1 and 2 (-27 to +23 mm/yr difference) and higher for scenario 3 (+178 mm/yr). PET is higher for all three scenarios (+34 to +108 mm/yr). Net precipitation (P-PET) is lower for scenarios 1 and 2 (-61 and -69 mm/yr respectively) and is higher for scenario 3 (+70 mm/yr). This contrast in scenarios is higher precipitation for scenario 3.

4.3 Simulation of past conditions with SWAT

The calibrated SWAT model was run using observed weather data from 1961 to 2017 with a daily time step (see **Figure 18** for results of the 1971-2017 period, the first 20 years are used as warm-up).

Results indicate that the major components of the water budget are the recharge and the real evapotranspiration (AET). Runoff represents only 9% of the precipitation (limited runoff on the sandy soils) on average while recharge represents on average 47% of precipitation. The average simulated recharge is 424 mm/year, AET is 367 mm/y, baseflow is 390 mm/y (0.79 m^3/s) and runoff is 72 mm/y. The difference between recharge and baseflow is caused by the uptake of shallow groundwater by ET and, to a lesser extent, by the recharge to the deep aquifer (in SWAT, once transferred to the deep aquifer, water cannot contribute to baseflow or ET).

At a finer timescale, the simulations show that recharge mainly occurs in the spring and fall. The recharge rate during these two periods can vary largely and some springs or falls can have recharge rates as low as that of some summers (**Figure 19**).

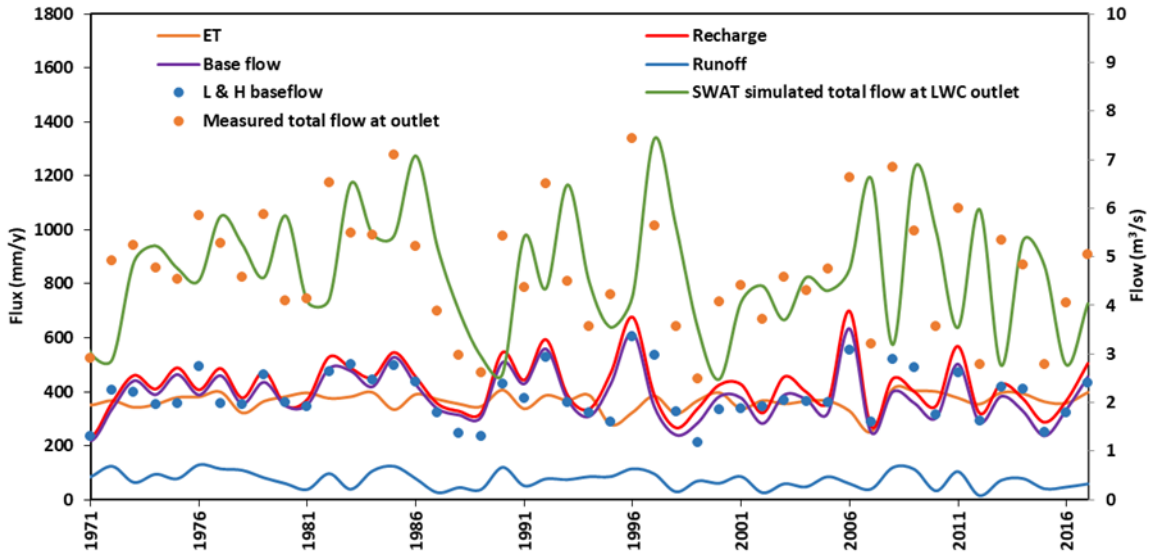

Figure 18. Simulated runoff, AET, recharge, Lyne and Hollick (1973) baseflows, and simulated baseflows from the SWAT model for the 1971-2017 period using observed precipitation and temperature. Measured flow at the outlet and simulated flow using SWAT model are presented on the secondary axis.

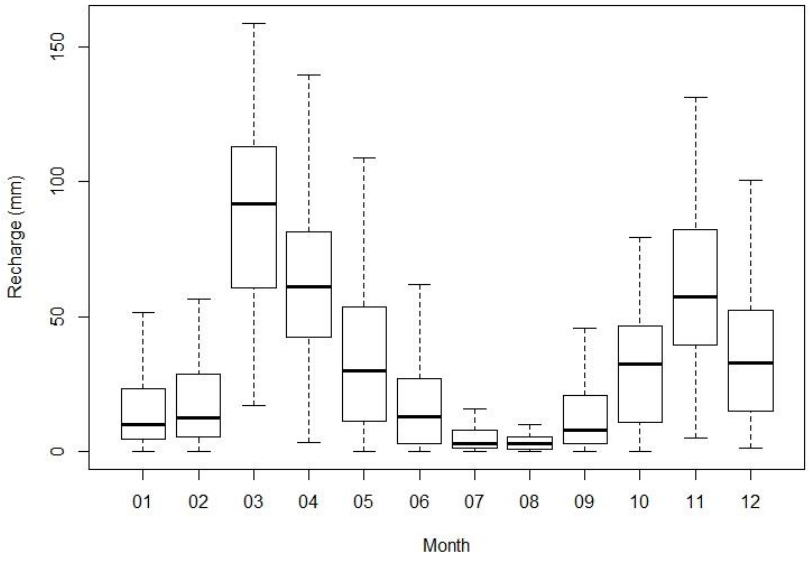

Figure 19. Simulated monthly recharge rates for the 1960-2017 period with SWAT.

4.4 Simulation of past conditions with MODFLOW

The impact of the regional flow of groundwater was assessed using the MODFLOW model. The average monthly recharge from the SWAT model for the 1960-2017 period was applied uniformly over the model domain with monthly stress periods. The main outputs from the model are the groundwater flow to the stream network and the difference between groundwater inflow and groundwater outflow at the west and east boundary conditions. **Figure 20** illustrates the variations in baseflow and the general head boundary conditions (difference between flow into the study area and flow out of the study area). The mean average baseflow is 320 mm/y (0.64 m³/s) and the average flow through the boundaries is -108 mm/year (more groundwater flowing out of the study area than groundwater flowing in the study area). This means that part of the aquifer recharge does not reach the river within the LWC, but flows underground towards the Grand River. However, this flow is not equal to the difference in baseflows simulated with the MODFLOW and SWAT models (70 mm/yr). This difference could be due to the uptake of groundwater by evapotranspiration which occurs where groundwater levels are close to the surface in SWAT but is not represented in MODFLOW.

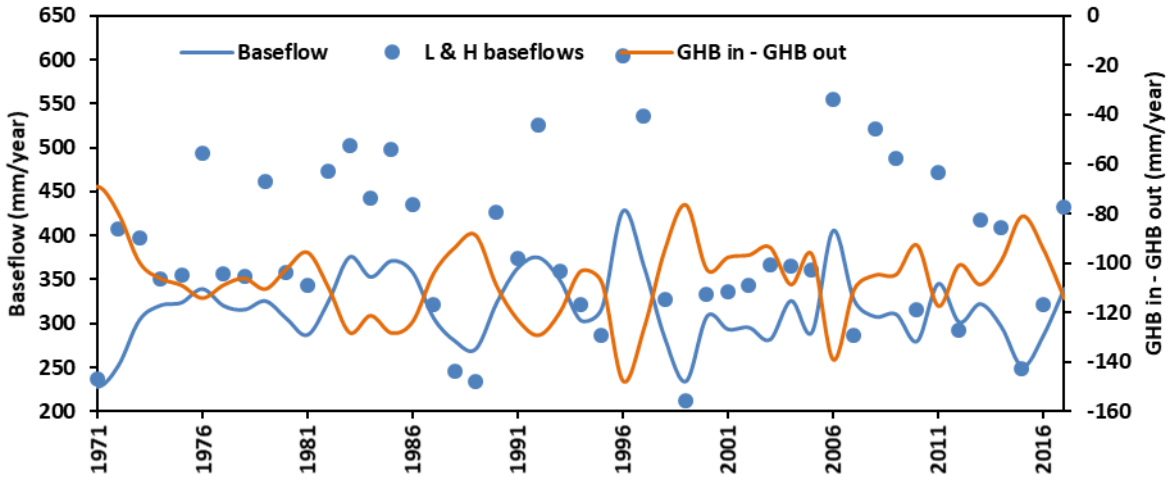

Figure 20. Simulated annual baseflows and regional flows (groundwater flowing in minus groundwater flowing out of the study area) from MODFLOW for the 1971-2017 period with SWAT-simulated recharge.

4.5 Simulation of past conditions with SWAT-MODFLOW

The calibrated SWAT and MODFLOW models were used in the coupled SWAT-MODFLOW model for simulation of the observed data from 1961 to 2017. The simulated flows compare very well with the measured flows at the LWC outlet (**Figure 21**). The model captures the inter annual fluctuations of the flows, including the more contrasted changes in flow rates from year to year since 2005. The simulated baseflows are much less variable than those obtained with SWAT and with MODFLOW (**Figure 22**), although the trends were similar. Since 1970, the groundwater elevation show relatively little interannual variations (**Figure 23**).

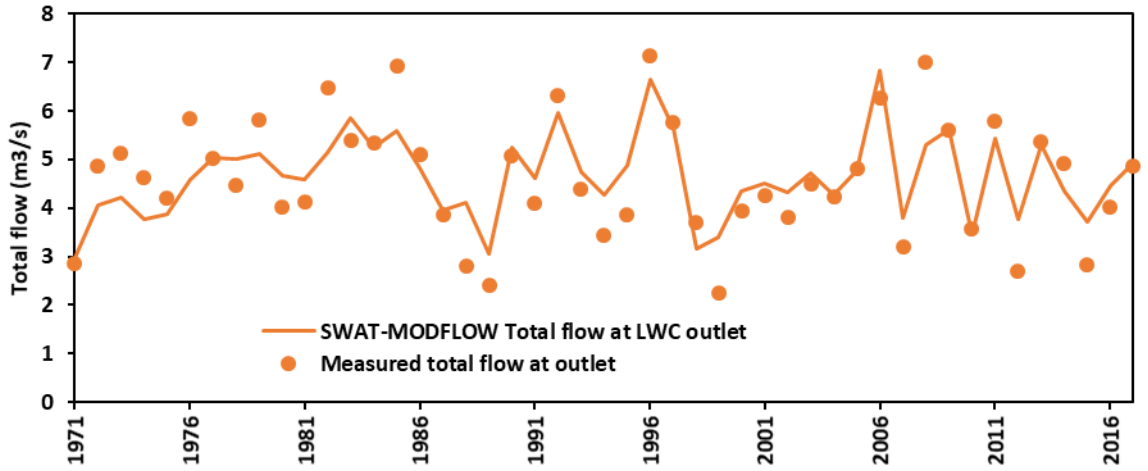

Figure 21. Measured and simulated annual flows at the outlet from SWAT-MODFLOW for the 1971-2017 period.

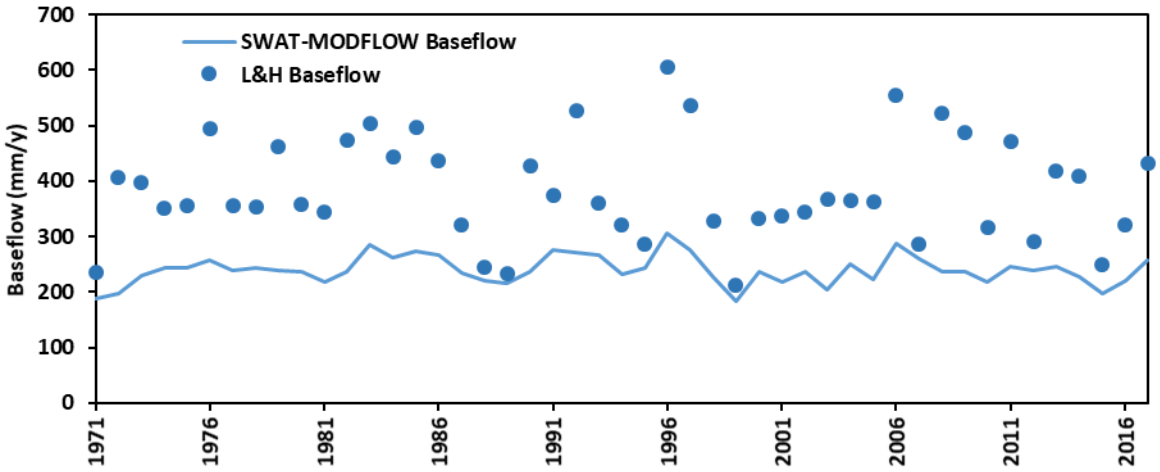

Figure 22. Simulated annual baseflows from SWAT-MODFLOW for the 1971-2017 period.

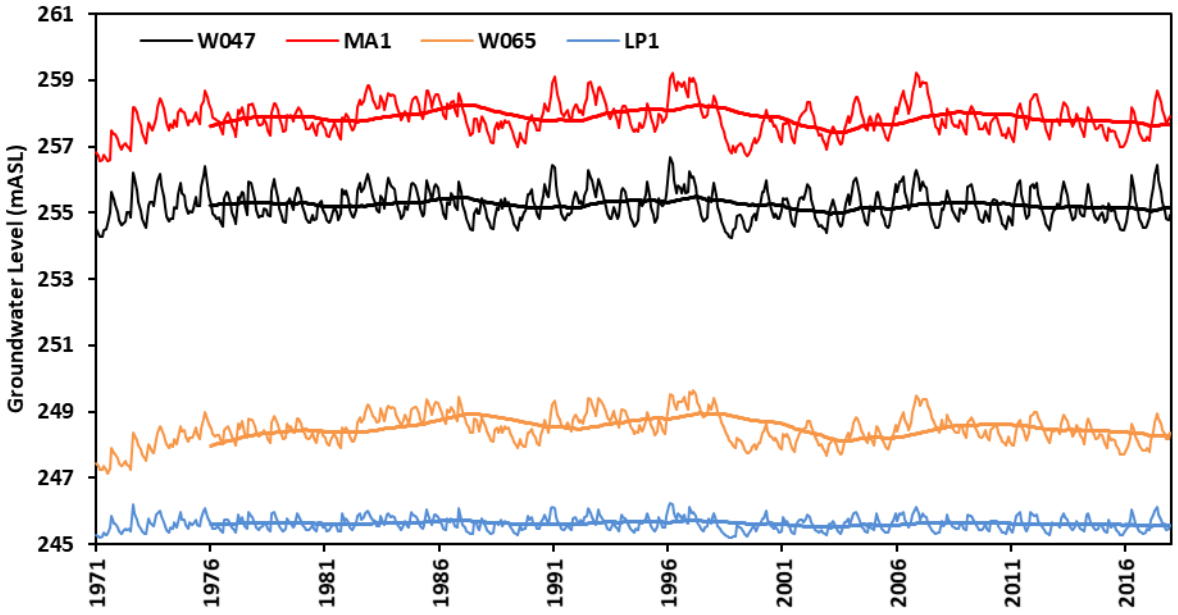

Figure 23. Simulated monthly groundwater levels from SWAT-MODFLOW for the 1971-2017 period.

4.6 Simulation of future conditions with SWAT and MODFLOW as separate models

Daily meteorological data from the three selected climate change scenarios were summarized at a monthly time step and incorporated as input into the calibrated SWAT model. The simulated recharge from the SWAT simulation was then averaged over the study area and used as recharge in the MODFLOW model.

The SWAT simulations show that there will be major changes in the seasonal pattern of the recharge. Recharge will increase during the winter months (~50 mm by 2100) and will decrease during the spring months (~20 mm by 2100). Fall and summer recharge remain stable except for scenario 3 for the fall months (~50 mm of increase by 2100) and lower recharge for scenario 1 in the summer (**Figure 24**). The simulated baseflows follow the same patterns (**Figure 25**).

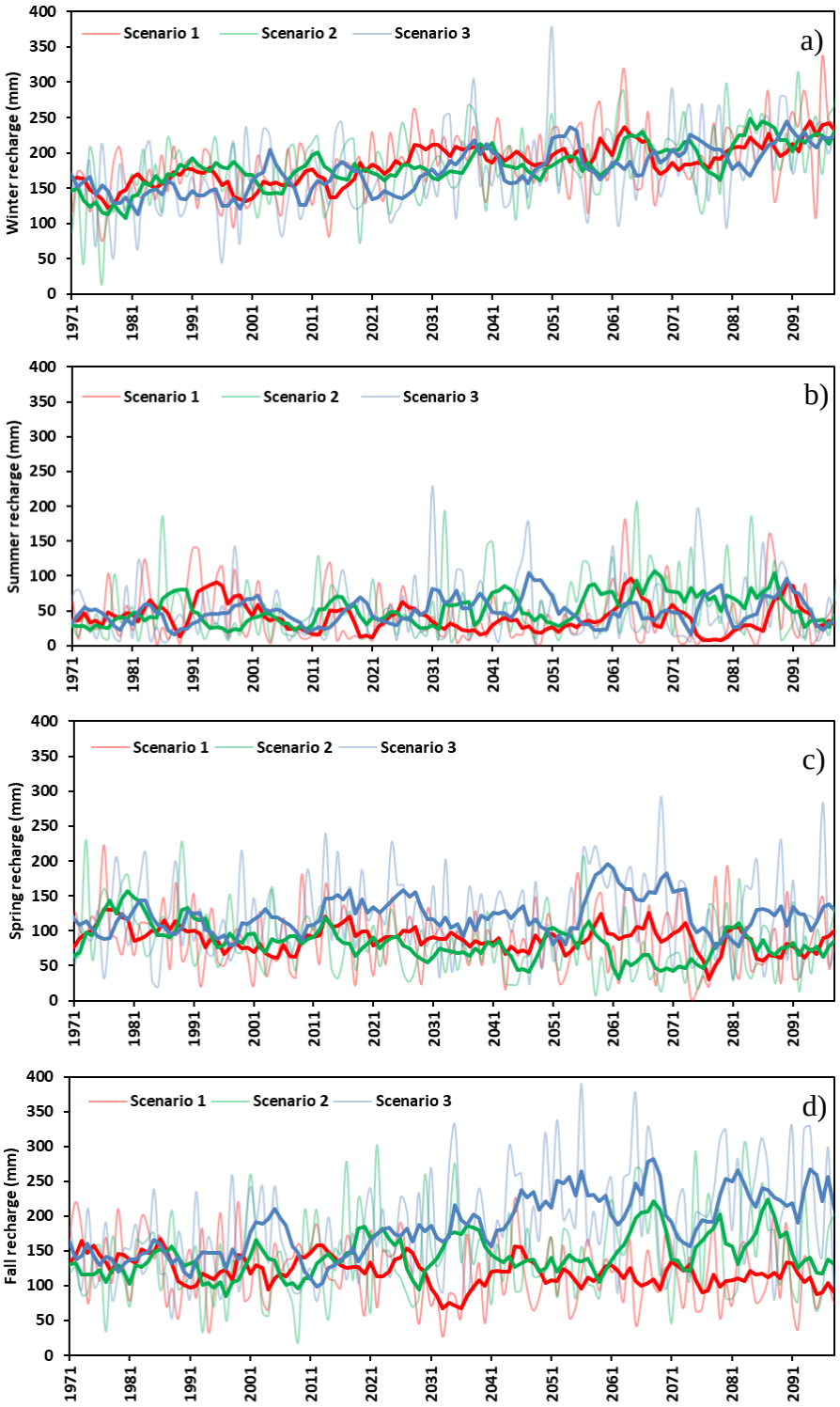

Figure 24. Simulated recharge from SWAT with precipitation and temperature date from the climate change scenarios between 1971 and 2100 for a) winter, b) summer, c) spring and d) fall seasons. The bold lines represent the 5 year moving average.

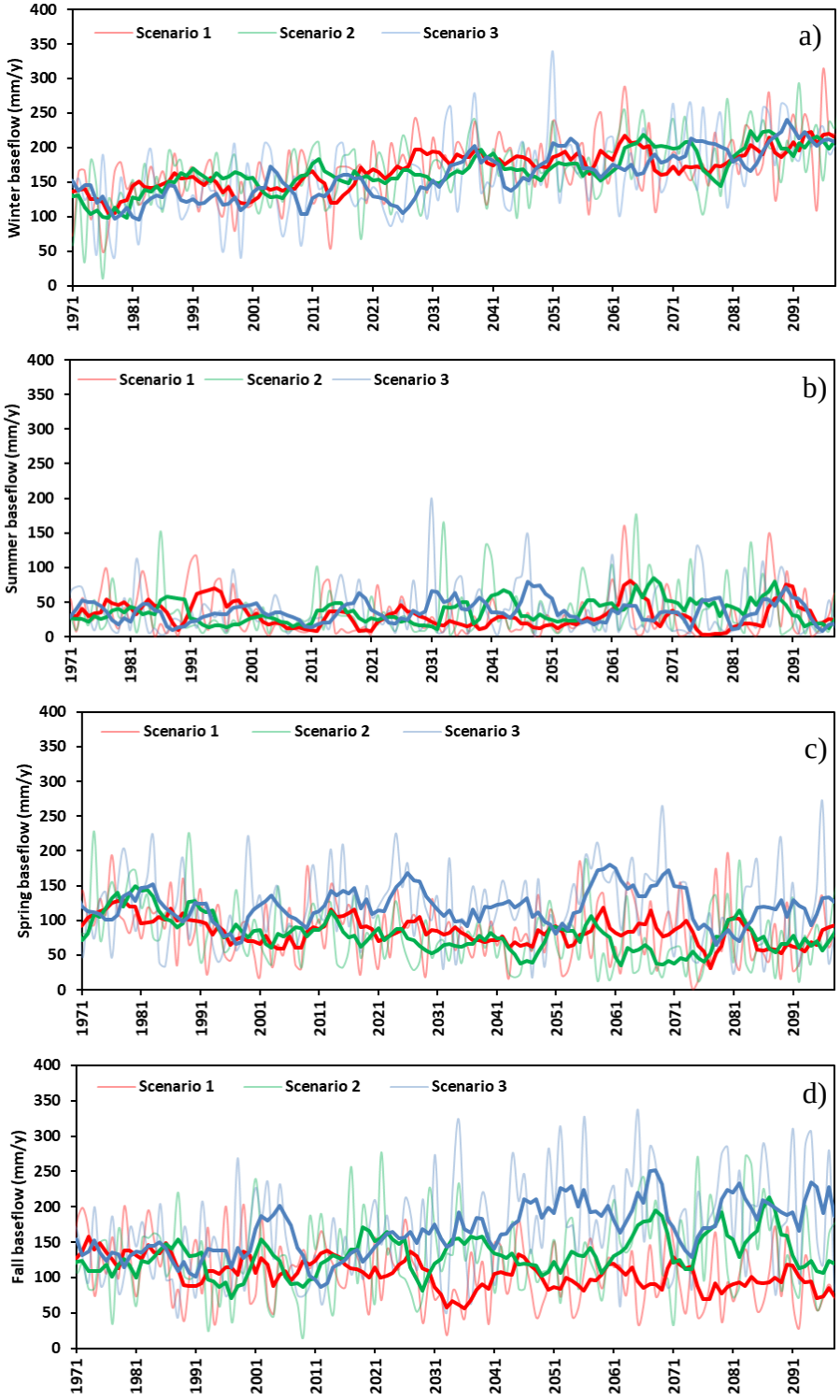

Figure 25. Simulated baseflows from SWAT with precipitation and temperature data from the climate change scenarios between 1971 and 2100 for a) winter, b) summer, c) spring and d) fall seasons. The bold lines represent the 5 year moving average.

Because the SWAT-MODFLOW simulations take a long time to run, the horizons selected to compare the results from the three models was twenty years, 1971-1990 for the reference period, 2031-2050 for the first future horizon and 2071-2090 for the second future horizon.

The SWAT modelling results indicated that the average recharge for the climate scenarios ensemble for the 1971-1990 period was 438 mm/year and was statistically significant from the future periods 2031-2050 and 2071-2090. The mean recharge for the future time periods was 482 mm/year and 513 mm/year, respectively (**Table 6**). The ensemble means for the baseflow showed that Scenario 1 and Scenario 3 were significantly different from each other; however, Scenario 2 was not significantly different from both Scenario 1 and Scenario 3. The mean values for the baseflows were 403 mm/year, 432 mm/year, and 462 mm/year for 1971-1990, 2031-2050, and 2071-2090 time periods respectively. Overall results suggest that both recharge and baseflows for the past conditions are significantly different from the further future conditions (2071-2090).

Table 6. Comparison of the different simulated time periods for recharge and baseflows from SWAT.

	Average recharge (mm/y)			
	Scenario 1	**Scenario 2**	**Scenario 3**	**Ensemble**
1971-1990	440[a]*	444[a]	431[a]	438[a]
2031-2050	415[a]	461[a]	570[b]	482[b]
2071-2090	428[a]	521[b]	594[b]	515[b]
	Average baseflow (mm/y)			
	Scenario 1	**Scenario 2**	**Scenario 3**	**Ensemble**
1971-1990	411[a]	414[a]	403[a]	403[a]
2031-2050	368[a]	413[a]	515[b]	432[ab]
2071-2090	382[a]	469[b]	535[b]	462[b]

* Different letters (exponents) indicates statistically different values from the other time periods within one scenario.

Groundwater elevations close to the River boundary condition (LP1) vary less than the wells located far from the boundary (**Figure 26**). Results from the simulations based on scenarios 2 and 3 indicated an increase in groundwater levels through time, while results from the simulation using scenario 1 indicated that groundwater levels could remain stable. Simulated baseflows from MODFLOW were smaller than the baseflows from the SWAT model. The ensemble means for the baseflow using the MODFLOW model showed that baseflow in all three time periods were lower than the SWAT model baseflow and all three time periods were significantly different from each

other (**Table 7**). The mean values for baseflow were 331 mm/year, 360 mm/year, and 385 mm/year for 1971-1990, 2031-2050, and 2071-2090 time periods respectively (**Table 7**).

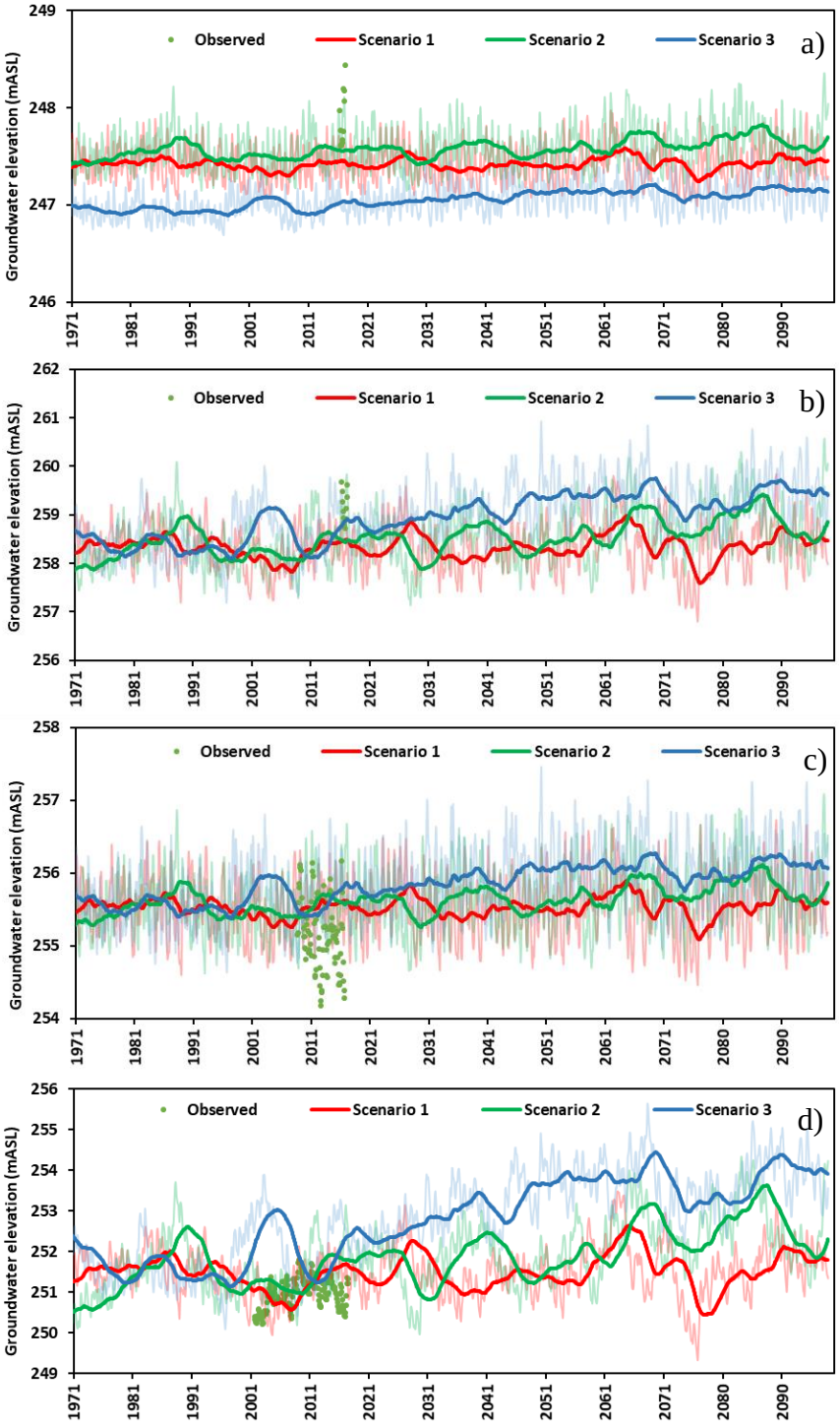

Figure 26. Simulated groundwater levels from MODFLOW for observation wells a) LP1, b) MA1, c) W047 and d) W065 observation wells. The bold lines represent the 5 year moving average.

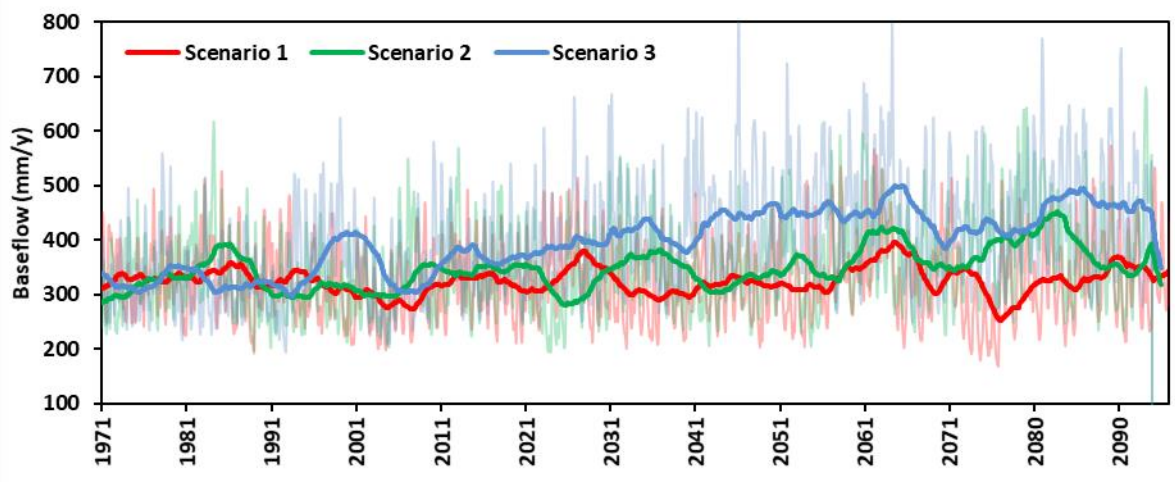

Figure 27. Simulated annual baseflows from MODFLOW with the SWAT-recharge derived from the three climate scenarios. The bold lines represent the 5 year moving average.

Table 7. Comparison of the different time periods for baseflows from MODFLOW.

	Average baseflow (mm/y)			
	Scenario 1	**Scenario 2**	**Scenario 3**	**Ensemble**
1971-1990	334[a]	334[a]	325[a]	331[a]
2031-2050	313[a]	345[a]	421[b]	360[b]
2071-2090	332[a]	391[b]	444[b]	385[c]

* Different letters (exponents) indicates statistically different values from the other time periods within one scenario.

4.7 Simulation of future conditions with the SWAT-MODFLOW model

The SWAT-MOFLOW model was run for three twenty-year time periods (1971-1990; 2031-2050; 2071-2090). The simulated SWAT-MODFLOW results based on the seasonal variations indicate that the winter recharge is increasing markedly in later years of 20th century (**Figure 28a**). Scenario 2 has the highest increase while Scenario 1 had the least increase during the winter months. Increased winter recharge could be due to higher temperatures during the winter months which induce early snowmelt. There was only a small change in the spring recharge during all three simulation periods (**Figure 28b**). Summer recharge has a decreasing trend in the late century compared to the past conditions (**Figure 28c**) which could be due to earlier snowmelt and reduced available water in the summer months. Fall recharge has an increasing trend similar to that of the winter recharge for scenarios 2 and 3 (**Figure 28d**). There was a slight decrease in the fall recharge for Scenario 1 (**Figure**

28**d)**. Heavy rainfall events during the fall months could be the main reason for the higher recharge rates during this season.

The annual baseflow increases for scenarios 2 and 3 for the two future periods while baseflow with scenario 1 remain approximately the same (

Figure 29). The results for the simulated SWAT-MODFLOW model for the groundwater elevation show that groundwater levels increase in the future compared to the past conditions for scenarios 2 and 3 (**Figure 30).** However, Scenario 1 has a slight decreasing trend for groundwater levels compared to past conditions (**Figure 30**).

The average recharge for the climate scenario's ensemble for 1971-1990 period was 442 mm/year and was statistically significant from the future period 2031-2050 with a mean recharge of 485 mm/year and 2071-2090 with a mean recharge of 513 mm/year (**Table 8**). However, the ensemble means for the baseflow showed that all three time periods were significantly different from each other with mean values of 251 mm/year (0.52 m^3/s), 271 mm/year (0.56 m^3/s), and 284 mm/year (0.59 m^3/s) for 1971-1990, 2031-2050, and 2071-2090 time periods respectively. Overall results suggest that both recharge and baseflows for the past conditions are significantly different from the future conditions.

Table 8. Comparison between the 1971-1990, 2031-2050, and 2071-2090 time periods for recharge and baseflows from SWAT-MODFLOW.

	Average recharge (mm/y)			
	Scenario 1	**Scenario 2**	**Scenario 3**	**Ensemble**
1971-1990	444[a]	450[a]	430[a]	442[a]
2031-2050	417[a]	471[a]	567[b]	485[b]
2071-2090	430[a]	523[b]	588[b]	513[b]
	Average baseflow (mm/y)			
	Scenario 1	**Scenario 2**	**Scenario 3**	**Ensemble**
1971-1990	251[a]	247[a]	253[a]	251[a]
2031-2050	241[a]	306[a]	266[b]	271[b]
2071-2090	246[a]	316[b]	290[b]	284[c]

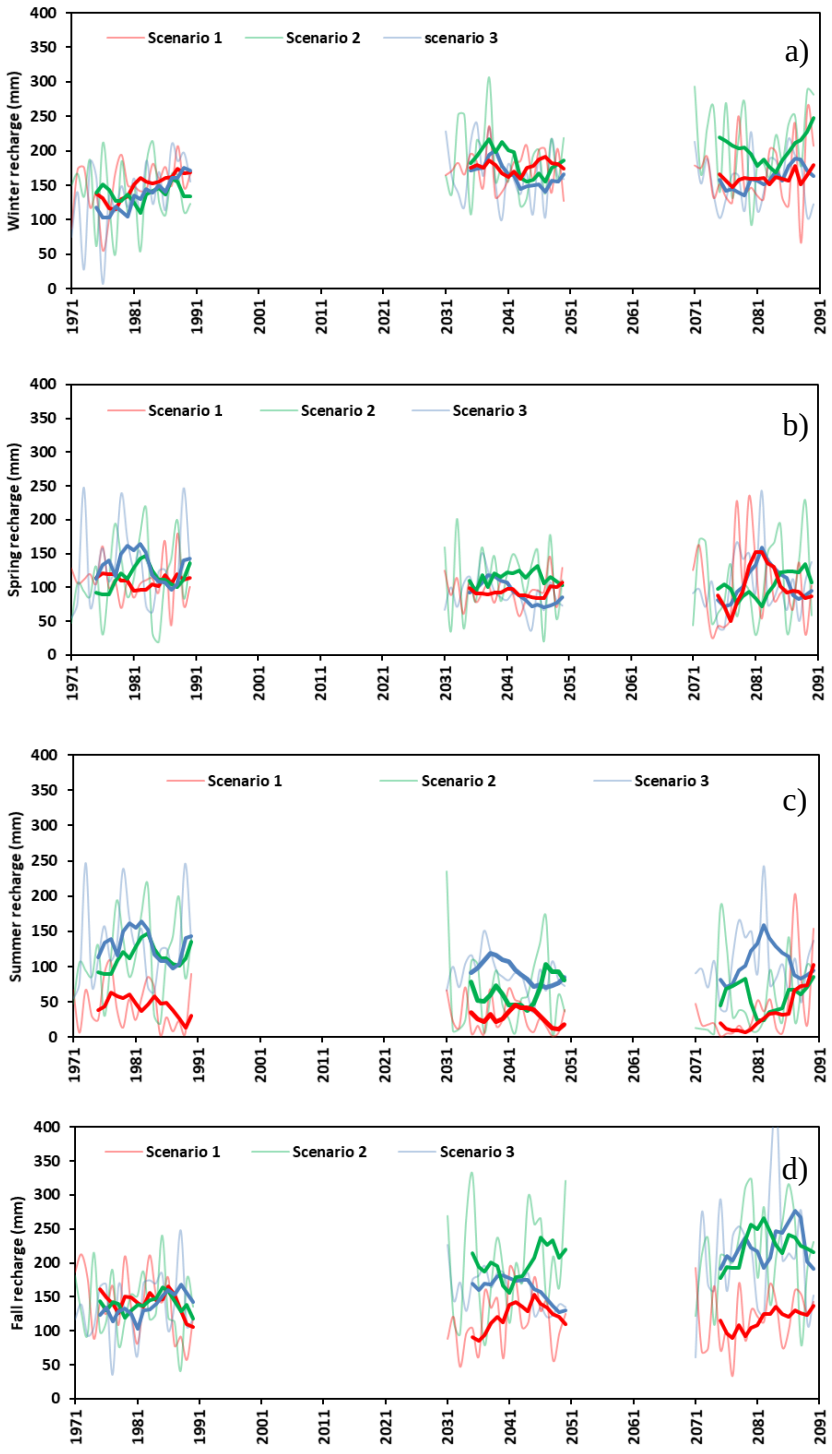

Figure 28. Simulated seasonal recharge from SWAT-MODFLOW for a) winter, b) spring, c) summer and d) fall with precipitation and temperature data from the climate scenarios for the reference and the two future periods. The bold lines represent the 5 year moving average.

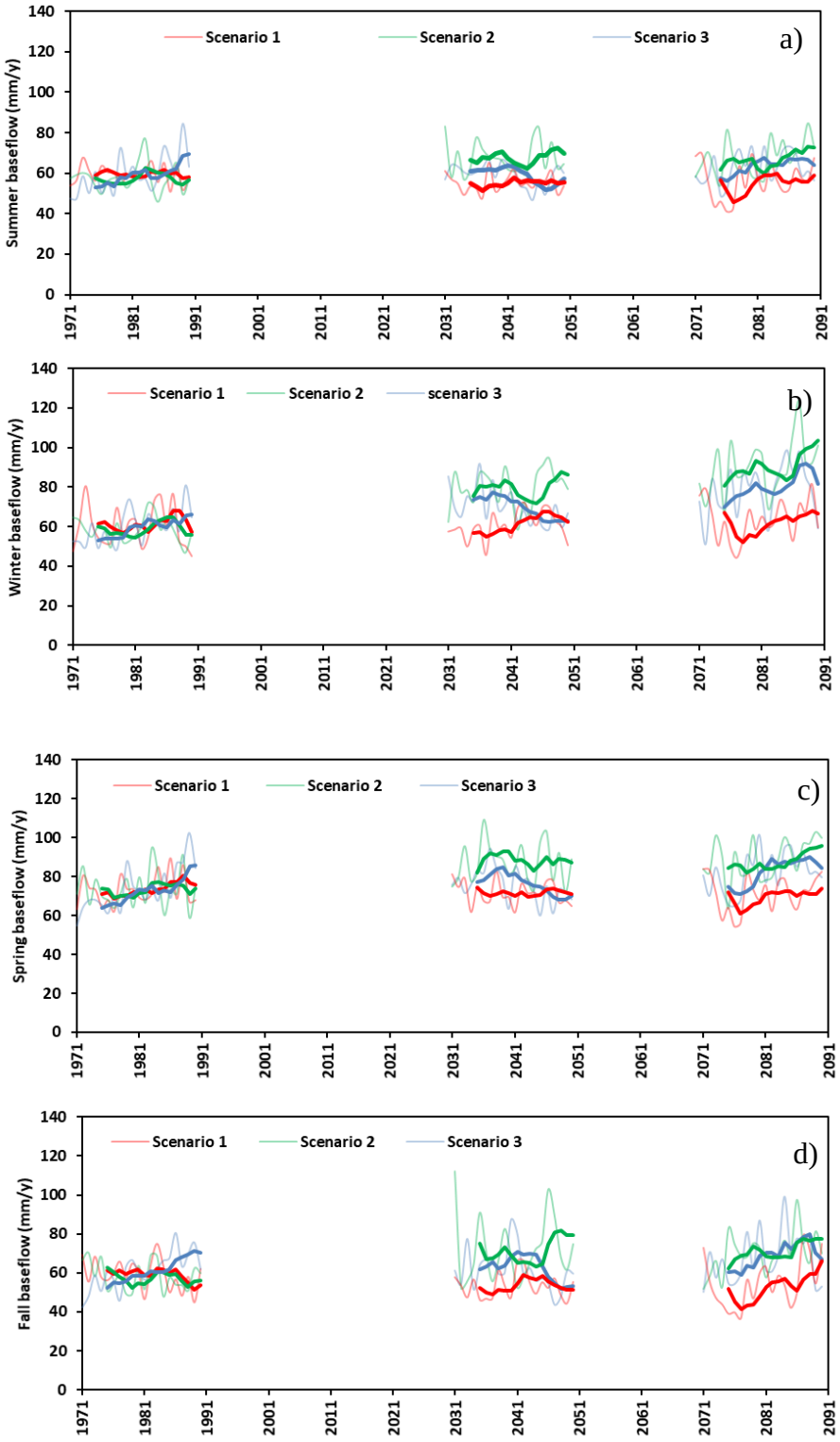

Figure 29. Simulated annual baseflows from SWAT-MODFLOW for a) winter, b) spring, c) summer and d) fall with precipitation and temperature data from the climate scenarios for the reference and the two future periods. The bold lines represent the 5 year moving average.

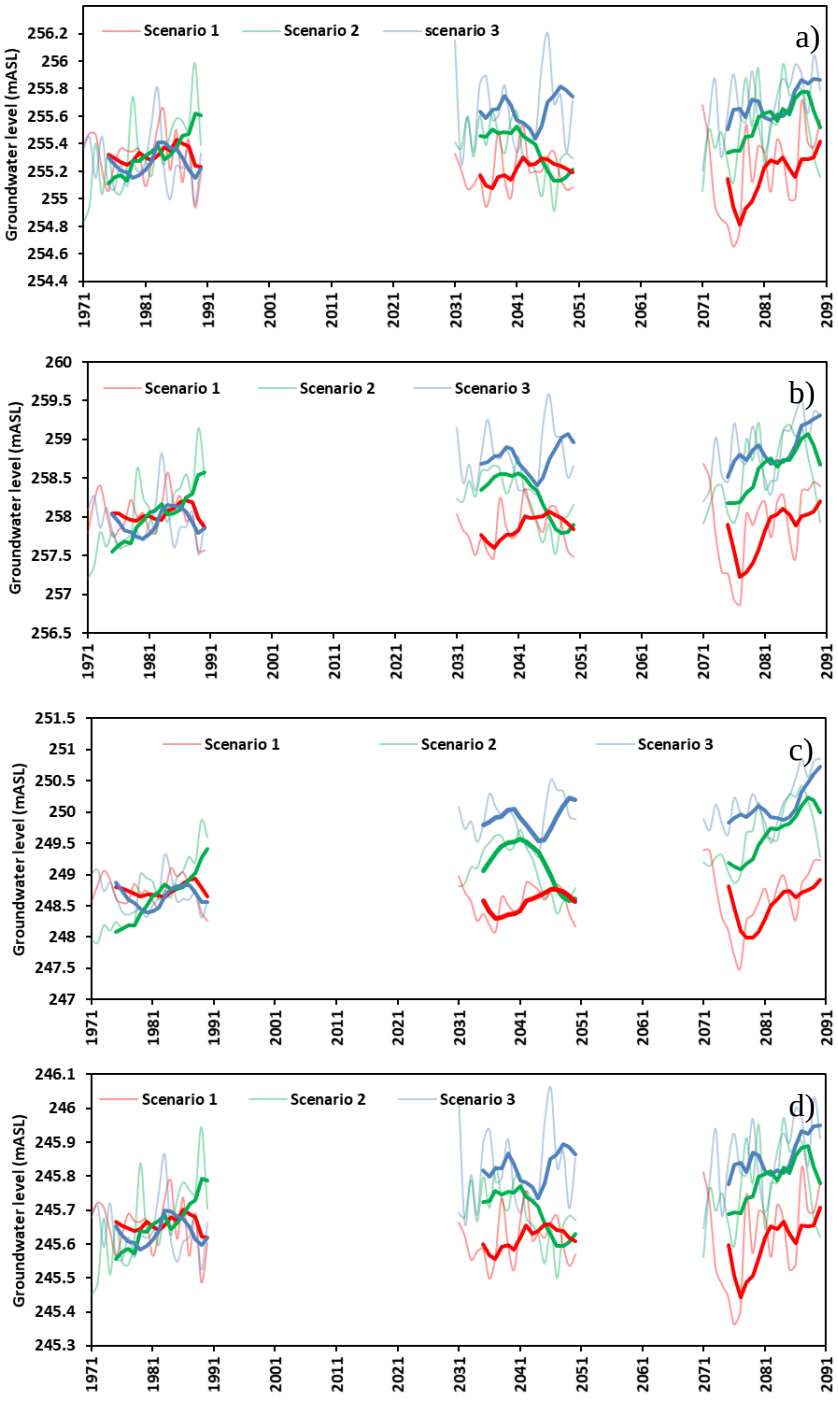

Figure 30. Simulated annual groundwater levels from SWAT-MODFLOW for observation wells a) W047, b) MA1, c) W065 and d) LP1 with precipitation and temperature data from the climate scenarios for the reference and the two future periods. The bold lines represent the 5 year moving average.

5 DISCUSSION

5.1 Uncertainties in the water budget and in the models

The approach used in this study was developed to assess as widely as possible, the range of available water for the recent past and for future conditions. To do this, the different terms of a water budget were first assessed based on available data and on newly acquired data. These water budget components are prone to errors and uncertainty linked both to measurement errors and to the methods used to quantify them.

Early in the project, it was decided that meteorological data extracted from the ANUSPLIN interpolated grid (10 km x 10 km grid; Environment Canada, 2018) would be used. This decision was made because there was no meteorological station located close to the study area that provided precipitation and temperature continuously since 1960. The widely used interpolated data provide a reliable and uninterrupted source of information that was crucial for the study of long-term past conditions. However, because they are based on a gridded interpolation, precipitation and temperature data extracted for the LWC are not exactly equal to those measured at nearby meteorological stations, thus introducing uncertainty in past data.

The method used to estimate potential evapotranspiration for the study area is that of Oudin et al. (2005). This method was selected because it uses only air temperature (and coordinates to determination solar radiation), an important criteria for the estimation of potential evapotranspiration for future conditions. Other methods using detailed meteorological variables would provide an assessment of the uncertainty associated with the Oudin et al. (2005) formula.

Recharge for the study area, estimated with the Lyne and Hollick (1973) baseflow separation method for the 1961-2017 period varies between 159 and 585 mm/yr with an interannual median (1961-2017) of 344 mm/yr. Also, using the difference between inflows and outflows from the study area measured 11 times in 2017 provides a lower value of 148 mm/yr which is similar to the lower end value of the recharge estimate based on baseflow separation. Having only one year of data is limiting to estimate recharge and having long term inflow measurements would provide a more reliable value. Using other approaches to estimate baseflows, either with other digital filters for baseflow separation or with natural tracers would provide a complementary assessment of recharge uncertainty. Using other

approaches to estimate recharge more directly, such as the water table fluctuation method, would be useful to further assess recharge uncertainty.

A more reliable estimation of current pumping rates (from all sources) for the study area would provide crucial information for the water budget estimation. In this work, the declared pumping rates since 2005 are very low and an order of magnitude below the allowed (permitted) volumes. Although these values may be realistic, more work is necessary to compare them with current irrigation practices in the study area. This information is required to fully understand the present impact of agricultural production on the water budget. The dichotomy between permitted (PTTW) amounts and the declared usage requires further investigation.

Three models were also used to assess available water for the recent past and for future conditions. The SWAT model is based on the hypothesis that all the water that flows in the subwatershed flows out at its outlet. The representation of groundwater flow in this model is also reduced to its simplest expression. Calibration of the SWAT model required the estimation of a large number of (often empirical) parameters. The MODFLOW model (as it was developed for the LWC) is based on the hypothesis that groundwater can flow in and out of the study area through its uphill and downhill boundaries. The representation of groundwater recharge is highly simplified as a time-dependant and spatially constant value imposed on the saturated zone (no representation of the unsaturated zone). Calibration of the MODFLOW model was based on head values available only for a ten year period.

These hypotheses and limitations are inherent to all surface flow and groundwater flow models. Use of the SWAT-MODFLOW model was intended to alleviate these limitations. Although the integrated model uses the parameters calibrated for the individual models, it includes an assessment of flow through the unsaturated zone as well as groundwater flow into and out of the study area, thus providing a more realistic representation of the entire water cycle on the LWC. However, running the SWAT-MODFLOW model over long periods was time consuming.

In this work, three scenarios of possible future precipitation and temperature data provided by the Ouranos Consortium were used to assess future water availability. Reducing the number of scenarios to three was considered necessary because of the expected combination with four land use change scenarios which would have produced a total of 12 scenarios to be run over a 150 year period. Although the three scenarios represent a large span of possible future climatic conditions, in hindsight

it appeared that including a larger number of scenarios might have provided more robust estimates of possible available water in the future.

5.2 Expected water stress

During the growing season, water is essential for plant growth. Sustaining sufficient ecological flows in LWC is also critical during the summer. Already for past and currently observed conditions, the available water in the LWC in excess of the potential evapotranspiration (PET) during the growing season is zero most of the time, except during very wet years (e.g. 2000). This indicates no or very little infiltration and recharge of the aquifer during the summer, with baseflow to the river likely driven by the slow decrease of groundwater levels in the sand aquifer which is replenished during the spring snowmelt period.

From the observed/historical data, the average permitted (PTTW) groundwater pumping rate is of similar magnitude to the average (past) recharge. Therefore, if pumping was to increase significantly in response to dryer conditions, for additional irrigation for example, the LWC could be at high risk of drying out during low flow periods.

The three selected climate change scenarios for the future period all predict increases in precipitation, temperature, and ETP. Furthermore, the three scenarios predict less water available (decreases in net precipitation from 53 to 98 mm/year) for the 2071-2100 period compared to the reference period on an annual basis.

The SWAT simulations indicate that there will be major changes in the seasonal pattern of the recharge in the future. Recharge will increase during the winter months (~50 mm by 2100) and will decrease during the spring months (~20 mm by 2100). Fall and summer recharge remain stable (except for scenario 3 for the fall months: ~50 mm of increase by 2100; and lower recharge for scenario 1 in summer.) The SWAT model results had a negligible change due to the suggested land use changes in the future. A primary reason for the negligible changes is due to the fact that none of the land use change scenarios examined major deforestation or urbanization for the study area.

The MODFLOW simulations highlight that groundwater elevations will likely increase in the future (scenarios 2 and 3), although results from scenario 1 indicate that groundwater elevations could

remain stable but with greater variations. The past and future modelling illustrates the importance of the study aquifer as a source of regional subsurface flow.

Future integrated (SWAT-MODFLOW) modelling indicates that the spring and the summer recharge have decreasing trends, meaning less water available during future growing seasons. The higher temperatures could also require more irrigation which could increase the ET, reducing groundwater elevations. The lower groundwater levels could consequently impact the baseflows in the LWC.

5.3 Recommendations

In Ontario, Permits to Take Water (PTTW) are currently issued on a site-specific basis. That is, in any given watershed or subwatershed, there is no limit on how much water can be approved or restricted. However, the province notes that existing conditions or stress are considered case-by-case for a review of new permits and permit renewals (Government of Ontario, 2005). This study has highlighted that a small subwatershed such as the LWC, with highly permeable soils, stresses on current water availability and dense agricultural activities, can be vulnerable to changes in the water budget for future conditions, and that current permitted water takings may not be sustainable into the future. However, the predictive coupled modelling does indicate that annual recharge will significantly increase into the future (2071-2100), potentially providing an opportunity for increased water use. Thus, the following recommendations can be used to improve water security in areas or catchments with high water demands.

- Water permitting processes should be considered on a small spatial scale such as on a subwatershed basis. This study has illustrated that a subcatchment such as the LWC can have permitted takings that are of similar magnitude to the recharge for the area. If everyone were to use their maximum permitted amount in this situation, there would be detrimental impacts on the stream hydrology and ecology. Water use reporting is critical for understanding the water budget. It is important that reporting mechanisms are used by all permit holders, and that the values being reported are fulsome and accurate.
- Future land use and climate changes can exacerbate these tenuous conditions. It is important that predictive models are used to simulate water budgets, including future impacts of climate and land use change when possible, to ensure collective uses do not have adverse impacts. Various types of modelling efforts (e.g. surface water: SWAT; groundwater: MODFLOW; or integrated models:

SWAT-MODFLOW) provide various levels of detail and information. For example, unlike SWAT, the MODFLOW results illustrate the importance of the regional flow in the subwatershed but at the same time, the model not take into account the uptake of groundwater by evapotranspiration. Integrated modelling allows for the investigation of the entire hydrologic cycle, including critical surface processes such as evapotranspiration. Integrated models would be a useful tool for water permitting purposes by provincial governments.

- Long-term monitoring of all components of the water budget is needed across high water use watersheds to build long-term datasets that can support holistic water management and the use of integrated modelling. This monitoring includes, in particular, infrastructure to measure flow rates and groundwater levels at multiple locations. Ongoing provincial and federal efforts such as the PGMN and Water Survey of Canada's real-time hydrometric data (gauging stations) are of critical importance.
- Policies that benefit water conservation in the agricultural sector should be implemented to mitigate future impacts of changing practices or land uses, especially in a changing climate. For example, if there is more irrigation to adapt to climate change in the future, more water will be lost to evapotranspiration. It will therefore be important to use truly effective irrigation technologies to limit this.
- Future research should incorporate land use change scenarios as greater knowledge about future crop trends becomes available. For example, best management practices and cropping systems that will better withstand extremes should be used, and drought resistant and flood-resistant crop varieties should continue to be developed and planted to withstand the future changes in temperature and precipitation.
- Future research should also focus on defining mitigation or adaptation measures for all components of the water cycle. For example, how, when and where can water be stored for critical periods in the summer? How can recharge areas be enhanced to increase groundwater storage? How can restrictions on water takings be developed in collaboration with farmers, especially during low flow periods? Which drought-resistant crops or changes in the agricultural calendar (e.g., earlier planting or later harvesting) would improve water storage and reduce climate change impacts?

6 CONCLUSIONS

This field and integrated modelling study examined the potential water available for agricultural production in a water-stressed, agricultural subwatershed in southern Ontario, the lower portion of Whitemans Creek (LWC), an affluent of the Grand River watershed. Field work to acquire new data and characterize the area and analyses of existing hydrometeorological time series provided important information that allowed the estimation of different components of the LWC water budget for past conditions. Land use changes since the 1950s were analyzed and possible future changes were considered. Past hydrological conditions were compared to possible future conditions under climate change to examine the evolution of the water budget in the study area. Future conditions were studied using a surface flow model (SWAT), a groundwater flow model (MODFLOW) and an integrated model (SWAT-MODFLOW).

The analysis of past and possible future hydrological conditions has shown that, overall, the groundwater system appears to be fairly resilient to climate change impacts. The results suggest that there are several opportunities for agricultural production based on possible increased water availability in the future. However, some challenges may occur due to the already stressed nature of the study subcatchment and due to the timing of future water availability in relation to agricultural production. The pertinent conclusions are as follows:

- Past water deficits (P-PET<0) have been observed for several years. Moreover, current permitted pumping (PTTW) is similar in magnitude to the average past recharge estimate. These water deficits could pose issues or conflicts for future water takings or increased irrigation needed for adaptation. However, the permitted water takings appear to be much higher than the declared ones. There is clearly a need to assess more precisely how much water (surface water and groundwater) is actually pumped in the study area.
- The three climate scenarios analyzed in this work indicate that future conditions could induce increased average annual temperature of 5.9^{o}C, and increased precipitation up to 174 mm/yr in the 2071-2100 time period. This could bring an increase in PET of 227 mm/yr and thus a decrease in annual net precipitation in the last decades of the end of the 21st century. Because this decrease occurs mostly during the growing season it could have a negative impact on different crops.

- The three models have shown that on average there will be more recharge, higher baseflows and higher groundwater levels in the subwatershed during the winter and fall seasons. However, the models show that there will also be less water available during critical crop periods such as lower recharge and baseflows in the spring and summer seasons. These changes in timing of water availability could have an impact on agricultural practices and could require more irrigation during the growing season.
- Combining land use change scenarios with climate change scenarios does not have much impact on the overall results as indicated in the SWAT model simulations for the 150 year period. The land use changes could impact the overall water balance if there was major deforestation, reforestation or urbanization in the study area. However, since land uses have been fairly constant in the study area over the last decades, these extreme conditions appear to be unrealistic in the future. Nevertheless, the need to shift agricultural practices because of possible changes in the timing of water availability might motivate the use of drought resilient crops.
- Comparing the three models was very useful to assess their respective capacities. The SWAT model requires many empirical parameters that need to be calibrated and does not represent groundwater flow to the stream nor possible groundwater inflows or outflows. However, it is easy to setup and run. The MODFLOW model relies on another model to estimate recharge, but explicitly represents groundwater flow based on relatively few parameters. It is relatively easy to setup and run. The SWAT-MODFLOW model provides a complete assessment of the entire water cycle and thus does not have the process limitations of the other two models. However, this integrated model is not easily setup and requires long run times, thus necessitating some technical expertise and high-efficiency computers.

This study provides new insight into past and future conditions at a local scale for a water-stressed subwatershed in rural southern Ontario. This information is valuable for long-term planning for farmers, processors, rural residents and policy makers. These results will be useful to guide watershed and government agencies towards measures to adapt water management policies in the near future to mitigate the impacts of a changing climate. This study also provides an example of combining field and mathematical modelling methods that can be used to assess long-term water availability in an

agricultural setting. The approach can be used in a wide range of similar conditions throughout the country for an improved understanding of climate change impacts on agricultural water resources.

7 ACKNOWLEDGEMENTS

The authors acknowledge funding for this research provided by the MAPAQ (*Ministère de l'Agriculture, des Pêcheries et de l'Alimentation du Québec* – Quebec Ministry of Agriculture) and OMAFRA (Ontario Ministry of Agriculture, Food and Rural Affairs) and additional support from the GRCA (Grand River Conservation Authority). The authors also acknowledge the participation of Ouranos who provided the climate change scenarios. Finally, the authors thank the members of the advisory committee for providing useful comments throughout this research.

8 REFERENCES

AAFC. 2018. Annual Crop Inventories. Retrieved September 18, 2017 from: http://open.canada.ca/data/en/dataset/ba2645d5-4458-414d-b196-6303ac06c1c9

AquaResource Inc. 2009. Integrated water budget report: Grand River watershed. Grand River Conservation Authority, 224 p.

Arnold J.G., J.R. Kiniry, R. Srinivasan, J.R. Williams, E.B. Haney, S.L. Neitsh. 2012. SWAT. Soil & Water Assessment Tool. Texas Water Ressources Institute.

Barthel, R., S. Banzhaf. 2016. Groundwater and surface water interaction at the regional-scale – A review with focus on regional integrated models. Water Resources Management 30: 1. https://doi.org/10.1007/s11269-015-1163-z

Bush, E., D.S. Lemmen. 2019. Canada's Changing Climate Report. Government of Canada, Ottawa, ON, 444 p.

Cuthbert, M.O., T. Gleeson, N. Moosdorf, K.M. Befus, A. Schneider, J. Hartmann, B. Lehner. 2019. Global patterns and dynamics of climate–groundwater interactions. Nature Climate Change 9: 137–141.

Doherty, J.E., R.J. Hunt. 2010. Approaches to highly parameterized inversion—A guide to using PEST for groundwater-model calibration: U.S. Geological Survey Scientific Investigations Report 2010–5169, 59 p.

EarthFX. 2018. Whitemans Creek Tier Three Local Area Water Budget and Risk Assessment: Risk Assesment Report. Prepared for Grand River Conservation Authority on behalf of Lake Erie Source Protection Region, 170 p.

Erler, A.R., S.K. Frey, O. Khader, M. d'Orgeville, Y.-J. Park, H.-T. Hwang, D.R. Lapen, W.R. Peltier, E.A. Sudicky. 2019. Simulating climate change impacts on surface water resources within a lake-affected region using regional climate projections. Water Resources Research, 55: 130–155.

Etienne, J. 2014. Grand River Watershed Water Management Plan. Water Demand Management: Meeting Water Needs in the Grand River Watershed. GRCA.

Expert Panel on Climate Change Adaptation. 2009. Adapting to Climate Change in Ontario. Accessed from: http://www.climateontario.ca/doc/publications/ExpertPanel-AdaptingInOntario.pdf

FAO. 2019. Crop Information. Retrieved June 1, 2019 from: http://www.fao.org/land-water/databases-and-software/crop-information/tobacco/en/.

Fortin, V., R. Turcotte. 2007. Le modèle hydrologique MOHYSE (bases théoriques et manuel de l'usager). Note de cours pour SCA7420, Département des sciences de la terre et de l'atmosphère, Montréal: Université du Québec à Montréal, 17 p.

Gaudin, A.C.M., T.N. Tolhurst, A.P. Ker, K. Janovicek, C. Tortora, R.C. Martin, W. Deen. 2015. Increasing crop diversity mitigates weather variations and improves yield stability. PlosOne https://doi.org/10.1371/journal.pone.0113261.

Government of Ontario. 2005. Permit to Take Water (PTTW) manual. Queen's Printer for Ontario, PIBS 4932e.

Government of Canada. 2017. Data extracted from: https://maps.canada.ca/czs/index-en.html

Government of Ontario. 2017. Well records. Retrieved November 14, 2017 from: https://www.ontario.ca/page/well-records

Government of Ontario. 2019. Water bottling rules and moratorium in Ontario. Retrieved August 1, 2019 from: https://www.ontario.ca/page/water-bottling-rules-moratorium-ontario.

Government of Canada. 2019. Annual crop inventory. Retrieved from:

https://open.canada.ca/data/en/dataset/ba2645d5-4458-414d-b196-6303ac06c1c9

Government of Canada. 2017. Daily 10 km Gridded Climate dataset 1961-2017. Retrieved from: ftp://ftp.nrcan.gc.ca/pub/outgoing/canada_daily_grids/

Green, T.R., M. Taniguchi, H. Kooi, J.J. Gurdak, D.M. Allen, K.M. Hiscock, H. Treidel, A. Aureli, 2011. Beneath the surface of global change: Impacts of climate change on groundwater. Journal of Hydrology 405(3–4): 532-560.

Harbaugh, A. W. 2005. MODFLOW-2005, the U.S. Geological Survey modular ground-water model – The ground-water flow process: U.S. Geological Survey techniques and methods 6-A16. Various pp. http://pubs.usgs.gov/tm/2005/tm6A16/.

Kim, N.W., I.M. Chung, Y.S. Won, J.G. Arnold. 2008. Development and application of the integrated SWAT–MODFLOW model. Journal of Hydrology 356(1–2): 1-16.

Kovacs, H. 2015. Whitemans Creek water conservation & drought contingency planning. Prepared on behalf of the Brant Federation of Agriculture. Grand River Conservation Authority, Cambridge, ON. 40 p.

Larocque, M., J. Levison, A. Martin, D. Chaumont. 2019. A review of simulated climate change impacts on groundwater resources in Eastern Canada. Canadian Water Resources Journal 44(1): 22-41.

Lyne, V., M. Hollick. 1973. Stochastic time-variable rainfall-runoff modelling. Aust. Natl. conf. Publ. (pp. 89-93). Perth, Australia.

Margat, J., J. van der Gun. 2013. Groundwater around the World. CRC Press/Balkema. 376 p.

Ontario Geological Survey. 1981. Aggregate Resources Inventory of Burford Township Brant County Southern Ontario. Toronto: Ministry of Natural Resources.

Ontario Geological Survey 2010. Surficial geology of Southern Ontario; Ontario Geological Survey, Miscellaneous Release--Data 128-REV ISBN 978-1-4435-2483-4 [DVD] ISBN 978-1-4435-2482-7 [zip file].

Ontario Ministry of Agriculture, Food and Rural Affairs (OMAFRA). 2019a. Agriculture in the Great Lakes Basin – Stewardship and Innovation. Retrieved July 4, 2019 from: http://www.omafra.gov.on.ca/english/environment/facts/gl_basin.htm

Ontario Ministry of Agriculture, Food and Rural Affairs (OMAFRA). 2019b. Field Crops. Retrieved November 19, 2018 from: http://www.omafra.gov.on.ca/english/stats/crops/

Ontario Ministry of Energy, Northern Development and Mines (MENDM) 2017. 3D Mapping of surficial Aquifers. Data downloaded from: https://www.mndm.gov.on.ca/en/mines-and-minerals/applications/ogsearth/3d-mapping-surficial-aquifers.

Ontario Ministry of the Environment (MOE). 2005. Permit To Take Water Manual. Government of Ontario, Queen's Printer for Ontario, PIBS 4932e.

Ontario Ministry of the Environment and Climate Change (MOECC). 2017. Well records. Retrieved from: https://www.ontario.ca/data/well-records.

Ontario Ministry of the Environment and Climate Change (MOECC). 2016. Permit to Take Water. Database obtained after a Freedom of Information and Protection of Privacy Act request.

Osman, A.R.M. 2017. Water use conflict: a characterization and water quantity study in an agriculturally stressed subcatchment in Southern Ontario. MASc thesis, University of Guelph, 190 p.

Oudin, L., F. Hervieu, C. Michel, C. Perrin, V. Andreassian, F. Anctil, C. Loumagne. 2005. Which potential evapotranspiration input for a lumped rainfall–runoff model? Part 2 – towards a simple and efficient potential evapotranspiration model for rainfall–runoff modelling. Journal of Hydrology 303: 290–306.

Qian B., S. Gameda. 2010. Canadian agroclimatic scenarios projected from a global climate model. 90th American Meteorological Society Annual Meeting, January 17–21, Atlanta, Georgia.

Ray, D.K., P.C. West, M. Clark, J.S. Gerber, A.V. Prishchepov, S. Chatterjee. 2019. Climate change has likely already affected global food production. PLoS ONE 14(5): e0217148.

Shifflett, S., H. Kovacs, A. Wong. 2014. Grand River watershed management plan. Agricultural irrigation: Forecasts for future water needs. Grand River Conservation Authority, Cambridge, ON. 35 p.

Simpson, H. 2015. Ground water - an important rural resource, understanding groundwater. Factsheet 15-041, agdex 716/552, Ontario Ministry of Agriculture, Food and Rural Affairs, 4 pp.

Smith, M., K. Cross, M. Paden, P. Laban. 2016. Spring — Managing groundwater sustainability. IUCN, Gland, Switzerland.

Statistics Canada. 2016. Census Profile 2016. Retrieved from :

https://www12.statcan.gc.ca/census-recensement/2016/dp-pd/prof/details/page.cfm?B1=All&Code1=350138&Code2=35&Data=Count&Geo1=DPL&Geo2=PR&Lang=E&SearchPR=01&SearchText=Burford&SearchType=Begins&TABID=1

Taylor, R.G., B. Scanlon, P. Döll, M. Rodell, R. van Beek, Y. Wada, L. Longuevergne, M. Leblanc, J.S. Famiglietti, M. Edmunds, L. et al. 2013. Ground water and climate change. Nature Climate Change 3(4): 322–329.

Wolf, A.T. 1999. "Water wars" and water reality: Conflict and cooperation along international waterways. In: Lonergan S.C. (eds) Environmental Change, Adaptation, and Security. NATO ASI Series (2. Environment), vol 65. Springer, Dordrecht.

Wong, A. 2011. Water Use Inventory Report for the Grand River Watershed. GRCA.